NASA CONTRACTOR REPORT 166337

NASA-CR-166337
19820016174

An Investigation of Rotor Harmonic Noise by the Use of Small Scale Wind Tunnel Models

Harry Sternfeld, Jr.
Edward G. Schaffer

CONTRACT NAS2-10767
April 1982

NASA CONTRACTOR REPORT 166337

An Investigation of Rotor Harmonic Noise by the Use of Small Scale Wind Tunnel Models

Harry Sternfeld, Jr.
Edward G. Schaffer

Boeing Vertol Company
P. O. Box 16858
Philadelphia, PA 19142

Prepared for
Ames Research Center
under Contract NAS2-10767

National Aeronautics and
Space Administration

Ames Research Center
Moffett Field California 94035

CONTENTS

ILLUSTRATIONS

List of Symbols

C_T/σ	Coefficient of Thrust/Rotor Solidity
D	Horizontal Distance from Aircraft Rotor Hub to Microphone
d_F	Diameter of Full Scale Rotor
d_M	Diameter of Model Rotor
D/L	Disk Loading ∿ Lb/Ft^2
h/d	h = Distance of Main Rotor Hub from Ground Plane d = Diameter of Model Main Rotor
H	Vertical Height from Aircraft Rotor Hub to Microphone
Hz	Frequencey ∿ Hertz
L_{FS}	Linear Distance from Full Scale Aircraft to Microphone
L_M	Linear Distance from Model to Microphone
Ms	Time in Milliseconds
M_T	Advancing Blade Tip Speed ∿ Mach
S	Lateral Distance from Aircraft Rotor Hub to Microphone
SPL	Sound Pressure Level ∿ dB
$\overline{SPL_M}$	Adjusted Model Sound Pressure Level - dB
SPL_M	Measured Model Sound Pressure Level - dB
ΔL	Adjustment for Microphone Location - dB
ΔR	Adjustment for Reverberation - dB
ΔV	Adjustment for Wind Tunnel Velocity - dB
ΔT	Delta Time
T/C	Blade Thickness/Chord Length
V_T	Blade Tip Velocity ∿ Ft/Sec

SUMMARY

A study was conducted to determine the applicability of using small scale powered helicopter models operating in non-anechoic wind tunnels to predict the sound pressure levels of full scale rotor harmonic noise components. The investigation included noise generation due to high tip speed effects, tandem rotor blade/vortex interactions, single rotors operating on test towers, and the interaction between main rotor vortices and tail rotors.

In all cases it was found that the pressure time history waveforms characteristic of different noise generating mechanisms were properly reproduced by the models. Corrections for microphone locations, acoustical reverberation, and tunnel wind velocity were developed. Application of these corrections to the model data were found to yield satisfactory correlation with full scale sound pressure levels except for the isolated single rotor where highly transient data, both model and full scale, precluded good agreement or absolute values.

INTRODUCTION

Rotor noise has long been an acknowledged problem with respect to limiting the potential which helicopters have to serve both the military and civil markets. Prior to 1979, there were no official exterior noise standards for helicopters which were, therefore, developed either without noise constraints or else to a target which was set by the designer. In 1979, a very significant event occurred. The International Civil Aviation Organization (ICAO) Committee on Aircraft Noise developed a standard for helicopter external noise which limits noise during takeoff, flyby, and approach to levels which clearly ensure that, in the future, noise considerations will play a greatly increased role in helicopter design.

One impact of this standard is to place a much greater emphasis on the importance of accurate rotor noise prediction, prior to construction and availability of the aircraft for full scale measurements, because what in the past might have been an unfortunate misprediction could, in the future, result in the inability of a helicopter to receive a type certificate, thereby barring it from sale to civil users. In order to ensure receiving certification the manufacturer is required to design the aircraft to meet a noise level which is below the actual certification limit.

Although constant effort is being directed at improving the accuracy of helicopter noise prediction, the evaluation of the prediction methodology is based on comparison with full scale data which, in itself, contains many variables. With the exception of a limited amount of data obtained by Schmitz (Ref 1) using an airborne microphone system, full scale data

contains many variables. First of all, constantly changing distance and directivity of the acoustic signal with respect to the microphone, along with Doppler shifted frequency, make evaluation difficult unless the aircraft position is known accurately. Secondly, atmospheric attenuation, turbulence, and terrain acoustical effects distort the signal. In addition, constant changes in rotor input from the pilot and/or automatic control systems continually upset the input conditions to which the rotor responds. Considering the above it is not surprising that support or condemnation of an analytical procedure may depend on the data with which it is compared.

A primary purpose of this study is to evaluate the use of small scale wind tunnel models, such as those used for performance and stability testing, as an investigative tool for studying and predicting rotor noise since the use of wind tunnel models would help to eliminate many of the problems described above. The Boeing Vertol Company has been making acoustical measurements, on most of its helicopter and rotor models in the Wind Tunnel since 1968. During those programs, techniques in measurement and data analysis have been developed and an acoustical calibration of the Boeing Vertol 20' X 20' Wind Tunnel has been performed. In addition, full scale data has been obtained on some of the configurations which were measured in model scale. This data can be used to evaluate the use of wind tunnel models for investigating and predicting rotor noise, as well as providing the basis for an examination of the generation of harmonic rotor noise. A second benefit of the validation of acoustical wind tunnel modeling would be the encouragement to use this approach to evaluate potential noise reduction configurations, particularly those of high technical risk. The cost of full scale flight testing are so high that often the more innovative ideas never receive a trial while the more conservative ideas, which are tried, are condemned for not achieving substantial results.

It should be emphasized at the outset that the study deals only with rotor noise components which occur as discrete multiples of blade passage frequency (harmonic noise) and not with broadband noise. Model studies of broadband noise in the wind tunnel would be considerably more complex because the averaging techniques used to separate model from wind tunnel noise, and pseudonoise due to air blowing over the microphone, do not preserve broadband noise data. More importantly models for broadband noise study should probably be Reynolds Number scaled. At the present time harmonic noise sources dominate the helicopter noise problems and the study will examine the following phenomena: Rotational noise due to fluctuating lift and drag airloads; impulsive noise due to high Mach number effects; and impulsive noise due to blade-vortex interactions. Each of these mechanisms has a distinct and identifiable acoustical signature as shown in Figure 1.

DATA ACQUISITION

Wind Tunnel

All of the model testing described in this report has been conducted in the Boeing Vertol V/STOL Wind Tunnel. The Tunnel, illustrated in Figure 2 has a closed circuit with continuous flow and speed capabilities from 0 to 240 knots. The 20 X 20 ft. test section can be configured as an open throat, slotted section, or closed section (Figure 3). In the open throat configuration the model is located in the test section plenum which has a diameter of 66 ft. and a height of 75 ft. Figure 4 shows a typical model installation, in the closed, slotted configuration, including wall mounted microphone brackets installed in typical locations. The test section and bellmouth walls are of steel with the remainder of the circuit concrete. No special acoustical treatment has been applied to any walls or turning vanes.

The microphone employed for wind tunnel data acquisition are Bruel and Kjaer type 4134 one half inch cartridges mounted on a 2619 cathode follower. The microphones are fitted with type UA-0386 nose cones and are oriented so that they point into the wind. Polarizing voltages for the condenser microphones are provided by type 2807 power supplies. The data is recorded on one inch magnetic tape by a 14 channel Sangamo Wide Band FM system using Dynamics 7704/PG preamplifiers and Dynamics 7509/PS DC amplifiers for signal conditioning and California Instruments Model 7500 oscilloscopes for monitoring recording voltages.

Prior to each test program each microphone/recording system was calibrated over the frequency range of interest by means of a Bruel and Kjaer Type 4142 Microphone Calibration Apparatus. The sensitivity of the system was checked daily by a Columbia SPC-10 calibrator which applies a 114B, 1000 HZ signal directly to each microphone cartridge.

FULL SCALE

Full scale data was recorded using either the same system described in the preceeding section (except that one inch microphone cartridges were used) or using Nagra Type III and IV portable tape recorders for data acquisition.

DATA REDUCTION

The two fundamental approaches to analyzing rotor noise are to make measurements of the pressure time-history radiated from the rotor or to perform a Fourier analysis on the time domain data in order to obtain rotor harmonic spectra in the frequency domain. Each type of data format has its own unique advantages and disadvantages which will be examined in greater detail, although data for each model/full scale comparison

discussed in the later sections of this report are presented in both formats.

Another issue which must be considered carefully is whether the data sample to be analyzed should be a short sample of 'instantaneous' data or a longer sample in which the data has been averaged over a specified time duration. One of the purposes of averaging is to enhance a repetitive signal which may be contaminated by random noise. This condition arises in a wind tunnel where the periodic noise is caused by the rotor under study and the non-periodic noise by the wind tunnel itself, and/or by pseudo-noise due to the air flow over the microphone. Figure 5 illustrates the effectiveness of data averaging in such a situation. Averaging in the time domain was performed using a Federal Scientific Model 129H, high dynamic range digital averager and in the frequency domain by a Federal Scientific Model UA-500A Ubiquitous Spectrum Analyzer.

Another possible reason for averaging data is if the source itself is varying and it is desired to obtain values which are representative of the level which occurs most of the time without being dependent on the subjective selections of the data analyst. An example of highly variable data is illustrated in Figure 6 and shows approximately one half second samples taken at various times during a measurement of a full scale and a model rotor each operating on a test stand in very low winds. The unsteadiness is due to intermittent blade-vortex interaction and it is interesting to note that in each case, a spread of about eleven dB was measured with waveforms varying from non-impulsive to highly impulsive. The effect of time averaging the model data is shown in Figure 7 which compares a thirty second averaged sample with an unaveraged sample which was selected as representative of the most impulsive section of each respective record. The figure clearly shows how the averaging process completely eliminated all indications of impulsiveness from the higher thrust (C_T/σ = .102) record. It is therefore very important to know what one is looking for before selecting the data reduction process and to be particularly cautious if the subject of interest is transient data.

Another situation where averaging techniques cannot be employed is flyby data of full scale aircraft. For example, even at the relatively low speed of 120 knots the aircraft displaces about 200 feet every second thereby changing level and directivity so rapidly that virtually instantaneous data at specific aircraft positions must be used.

DATA ADJUSTMENT

General Approach

In order to achieve successful acoustical modeling, the following model design and operating conditions should be met:

Geometric similarity of rotors (number of blades, aspect ratio, planform, airfoil, twist).

Model should operate at full scale tip Mach number.

Model should operate at full scale advance ratio.

Model should operate at full scale $\frac{c\tau}{\sigma}$

Satisfying the above conditions will, for example, result in similar predicted rotational noise (Ref. 4), thickness noise (Ref. 5) and blade-vortex interaction noise (Ref. 6) regardless of the magnitude of the dimensions, provided that the location of the prediction point is also scaled to the full scale location.

Given the above similarities, the following equation expresses the adjustments which then must be made to the model data:

$$\overline{SPL_M} = SPL_M + \Delta L + \Delta R + \Delta V$$

where:

$\overline{SPL_M} \triangleq$ Adjusted Model Sound Pressure Level - dB

$SPL_M \triangleq$ Measured Model Sound Pressure Level - dB

$\Delta L \triangleq$ Adjustment for Microphone Location - dB

$\Delta R \triangleq$ Adjustment for Reverberation - dB

$\Delta V \triangleq$ Adjustment for Wind Tunnel Velocity - dB

Adjustment for Microphone Location

Microphones located in wind tunnels are constrained to fairly close proximity to the rotor because model rotors are generally sized so that they are of the order of one half of the cross dimension, located about mid-height in the tunnel, and most tunnels have lengths of from two to four times their width. Microphone locations for full scale out of doors measurements are generally selected further from the rotor if for no other reason than to minimize downwash effects. Figure 8 illustrates the typical range of locations involved. Obviously it

is ideal to have the model microphone at the same distance (measured in rotor diameters) as the full scale data. Unfortunately this arrangement is rarely possible. For purposes of this study, microphone locations were selected so that the directivity angle θ was as similar as possible. In the case of full scale flybys θ is a function of the approach distance D and was used as a basis for selecting the point in time at which full scale data would be read. In identifying this time on a magnetic tape recording, the time required for the sound to travel from the aircraft, when it was located at distance D, along ray line θ to the microphone should be included when correlating recording time with aircraft physical location.

Selection of the corresponding full scale distance, D, based on matching the elevation angle θ also defined the azimuth angle ψ which did not necessarily agree as well. In the case of tip speed effect data typical model data azimuth angles were approximately 20° from forward while full scale data was approximately 5°. Using the level flight data of Reference 1 as a guide this would be expected to introduce an error of less than 1 dB. A similar situation exists with respect to the data used to evaluate blade-vortex interaction effects where the low speed descent data from Reference 1 also indicates a small error. In both cases the sensitivity of the change in sound pressure level to elevation angle appears to be greater than the sensitivity to azimuth for the range of directivities involved. For isolated hovering rotors azimuth has no meaning and does not apply.

Figure 9 from Reference 3 shows the levels of several harmonics of a level measured by microphones located along a single ray line from the rotor. From this Figure it is apparent that beyond one diameter from the center of the rotor the attenuation closely followed the classical spherical spreading law. Although the near field drop off rate was considerably higher, all microphones used in this study were greater than one diameter and therefore:

$$\Delta L = 20 \log \frac{L_{M/dM}}{L_{F/dF}}$$

where L_M = Linear distance from model to microphone
L_F = Linear distance from full scale aircraft to microphone
dM = Rotor Diameter - Model
dF = Rotor Diameter - Full Scale

Adjustment for Reverberation

The purpose of the reverberation adjustment is to correct the model data acquired in the hard walled wind tunnel to values which would be expected if the equivalent wind tunnel data had been taken in the free field. Prior to this program, the Con-

tractor had performed such a calibration using the arrangement shown in Figure 10. Several microphones were mounted on a supporting structure such that they could be located at several stations throughout the wind tunnel. A single, control, microphone was kept at a fixed location four feet directly in front of the loudspeaker which was used as a noise source. Tests were conducted with tunnel slots installed and removed using sine waves, broadband noise, and recorded model rotor noise as input. The entire setup was then moved out of doors, to a large open field, and the procedure was repeated. Only one half of the tunnel width was surveyed since the structure is essentially symmetrical.

Figure 11 shows some typical results of these calibration procedures and indicate a reverberant amplification which is essentially independent of frequency but is sensitive to the tunnel configuration. An analytical prediction of the sound pressure which relates the buildup in a large room to a "Room Constant" was performed using the method described in Section 10.14 of Reference 2. The room constant (R) is defined as

$$R = \frac{S\bar{\alpha}}{1-\bar{\alpha}}$$

where: S = Total area of boundaries of room in sq. ft.

$\bar{\alpha}$ = Average energy absorption coefficient of the surface of the room

$$\bar{\alpha} = \frac{\alpha_1 S_2 + \alpha_2 S_2 + \ldots \alpha n Sn}{S}$$

where

$\alpha_{1,2,n}$ = Absorption coefficient of particular absorbing areas

$S_{1,2,n}$ = The surface areas corresponding to $\alpha_{1,2,n}$

In the case of the steel walled wind tunnel it can be assumed that there are two types of surfaces, the steel walls with α=0 and the ends and slots with α=1. Figure 11 also shows the results of predictions for the Boeing Vertol Wind Tunnel. Since the values of absorption coefficient for steel and air are not very sensitive to frequency, this explains the flat shape of the calibration curves. It is also noted that the analytically predicted buildup is in fairly good agreement with the measured values.

Adjustment for Tunnel Wind Velocity

Consideration should also be given to the effects which the velocity of the air flow in the wind tunnel might have on

noise propagation from the model to the microphone. In order to investigate the importance, if any, of this phenomenon a loudspeaker was placed in the tunnel and the sound pressure levels measured at several microphone locations for several wind velocities. The loudspeaker selected was a folded horn of metal construction which is designed such that the air flow could not impinge directly on the driver diaphragm. Pure tones and a recording of model noise were used as input signals. The test setup and a typical set of results are presented in Figures 12 and 13. The limiting velocity of about 250 feet per second was determined by the onset of visible speaker vibration. It is not suggested that these curves be applied to other wind tunnel installations but rather to point out that the effect of tunnel wind velocity should be considered and that a relatively simple calibration can be performed. It was initially expected that the effect, if any, would be increasing attenuation with increasing velocity. It is noted, however, that this was not always true, especially of the more distant microphones at higher frequencies. At the present time, no explanation of these effects is readily evident.

Atmospheric and Ground Attenuation - Full Scale Data

It should also be kept in mind that the full scale data might be affected by the atmosphere and ground terrain corrections for these types of propagation effects can be found in several publications such as References 7 and 8. Considering that all full scale measurements had been made over ground with very short cut vegetation and at distances no greater (and usually less) than two thousand feet, it is not surprising that attenuation over the frequency range up to 300 Hz, which would encompass at least the first twenty harmonics of most helicopters, is negligible. The corrections for atmospheric turbulence, discussed in Reference 7, appeared to provide too much attenuation which only indicates that the degree of small scale turbulence inherent in the Reference 7 curve was greater than that existent at the sites and times at which the full scale measurements were made. Since the conditions for acoustical measurements of helicopter noise are specifically limited to low wind and gust conditions, the results are probably not too surprising. In summary, no corrections have been made to the full scale data in this investigation.

Application to Data in the Frequency Domain

Figure 14 illustrates the adjustments which were discussed in the previous section applied to the harmonic spectrum of a model rotor operating, in hover on a test stand, in the wind tunnel while Figure 15 compares the adjusted data with full scale measurements. Figures 16 and 17 present similar comparisons for a helicopter in high speed forward flight. The detailed correction values are presented in Appendix A, Tables A-1 and A-2.

In both cases the general trending of harmonic sound pressure levels is quite good except that the full scale isolated rotor data displays significantly higher amplitudes in the fifth through ninth harmonics not apparent in the model data. In view of the variability in data measured on hovering rotors, which is discussed previously and illustrated in Figure 6, these comparative results are to be expected. In the forward flight case the model signal is stronger and more regular and the match between adjusted model data and full scale data is even better.

Application to Data in the Time Domain

Although the examples of the preceding section essentially bracket the goodness of fit, presentation and evaluation of data in the frequency domain format is extremely complex and laborious to describe, particularly if one is trying to compare two configurations or conditions. Although the harmonic spectra are of importance to the researcher, the results of wind tunnel tests will be of little use unless they can be expressed as single numerical values.

Figure 18 illustrates the above point by comparing the full scale data of a helicopter flying at four advancing tip Mach numbers achieved by varying rotor speed. The data is presented in both the frequency domain (spectra) and time domain (waveform). While the spectra show the increase in higher harmonic content with increased Mach number the picture tends to be a qualitative one because at Mach = .935, for example, over one hundred harmonics are depicted, with many more above 2,000 Hz. The peak-to-peak amplitude of the waveforms however, is a single value which grows as depicted in Figure 19 and yields information which is much simpler to evaluate such as absolute values, slopes, and significant divergence at Mach = .926.

The sound pressure levels used in the remainder of the report are peak-to-peak levels, while waveforms and spectra are presented as aids in further evaluating and identifying the predominant noise generating mechanisms.

If measurements are made in the time domain it is not necessary to correct the data for reverberation because it is possible to separate the directly radiated signal from its reflections as illustrated in Figure 20. Since the reflected paths will always be longer than the direct one, the combination of attenuation due to distance along with a small amount of energy loss at the reflecting surface, will serve to ensure that a peak-to-peak measurement will give the correct value for the directly radiated signal. An aid in identifying other paths and their associated time delays can be achieved by making a sharp impulsive noise at the model location and measuring the time delay of the several reflections. Figure 21 shows the results of such a test firing in the contractors wind tunnel. Although various techniques may be employed for

such measurements the example shown employed a high intensity electric spark as the source and the specialized instrumentation indicated in Figure 21 to make the precise measurement required relatively simple. Knowledge of the physical dimension involved, and the speed of sound can then aid in identifying the reflecting surfaces. Checks of this type can help to avoid the singular situation which could contaminate peak-to-peak data, when a reflected path arrives at the microphone with a delay time equal to the time between blade passages. If such a situation occurs, the microphone should be moved or acoustical absorption added to the reflective area.

EVALUATION OF RESULTS

In this section adjusted model data and full scale data will be compared on three bases, peak-to-peak amplitudes, wave forms, and spectra. As discussed in the preceeding section, peak-to-peak amplitude will be the primary quantitative measurement. The waveforms may be compared for shapes which are characteristic of the rotor noise generation mechanisms as depicted in Figure 1. In order to permit inspection and comparison of shapes over a substantial decibel range the linear waveform amplitudes have been approximately normalized and should not be scaled.

The spectra are most informative when viewed in terms of decay envelope. In general, the flatter the decay, the more impulsive the quality of the sound. In most cases, the spectra and waveforms are presented for two comparable sets of operating conditions which are indicated as circled points on the amplitude plots.

Tip Speed Effects

It has been well documented in such papers as Reference 9 that the acoustical radiation of a rotor operating at high tip Mach numbers becomes dominated by an unsymmetrical "N" wave (Figure 1) which increases in intensity as the mach number increases. All model tests were conducted using the Boeing Vertol Dynamic Rotor Test Stand (DRTS) shown in Figure 22a. Full scale data was measured on the Boeing Vertol Model 347 helicopter (Figure 22b). This aircraft was an experimental derivative of the CH-47 helicopter had an elongated fuselage and increased height aft pylon which virtually eliminated blade-vortex interactions in forward flight, thereby making it a good vehicle for investigating tip speed effects. Comparative model and full scale data were obtained with six percent thickness ratio tips (Figures 23a, b, c) and ten percent thickness ratio tips (Figures 24a, b, c). A single flight data point, corresponding to model data was also measured on the YUH-61 a single rotor helicopter (Figure 22c) and is presented in Figures 25a, b, c.

All comparative model and full scale data points agree within five dB with most showing no worse than two dB deviation, while the model waveforms clearly show the growth of the "N" wave which is characterized in the full scale data. Comparison of the spectral envelopes reveal an even more interesting correlation in that while both model and full scale envelopes display the expected decay from the fundamental at low mach numbers they both show maximum sound pressure levels in the range of the third to sixth harmonics with the first two harmonics substantially lower. This faithful replication of spectral detail is most encouraging.

Figure 26 illustrates the use of the model in high speed rotor blade development and compares a constant thickness blade with a thin tip and a blade which starts its taper at further inboard. The lack of separation below M_T = .80 indicates that rotational noise is dominating the signature while the separation above M_T = .85 gives evidence that contributions to thickness noise are being generated substantially inboard of the tip.

Isolated Rotors

The problems of large magnitude variations of transient sound pressure levels which are encountered when operating isolated rotors in very low winds have been discussed in the data anslysis section of this report. In accordance with that discussion, the amplitudes and waveforms presented in this section are based on the sampling method and represent the more impulsive portions of the data. All full scale data was measured on the Boeing Vertol Report Test Tower and the models on one of several test stands such as the one illustrated in Figure 27.

Comparison of model and full scale data are presented for three different rotors: the YUH-61A rotor (Figures 28a, b, c) which is forty-nine feet in diameter and has an advanced airfoil which changes spanwise in three stages with an outboard section t/c of 6%; the Model 347 rotor (Figures 29a, b, c) which is sixty feet in diameter and utilizes four CH-47C cambered airfoil rotor blades with a tip thickness of 10½%; and the YUH-62 (HLH) rotor (Figures 30a, b, c) which has a diameter of ninety-two feet which uses two spanwise sections of airfoil which are the same as the two inner sections of the YUH-61A with the outboard section thickness 8%.

First order least square lines have been shown on the amplitude plots in order to aid trend evaluation. It is apparent that although the absolute agreement of model and full scale data for the YUH-61A is quite close the full scale data for the Model 347 rotor exceeds the corrected model data by about 8 dB and by 10 dB for the YUH-62 rotor. A possible explanation may be that while the microphone location for the YUH-61 rotor was approximately four rotor diameters distant from the

center of the tower, the Model 347 locations were 1.8 diameters and the YUH-62 .85 diameters. It is also noted that the latter two microphones were in locations of high downwash. It is significant, however, that the slopes of the model and full scale least square fit lines are in very good agreement with each other and, in fact, vary very little between all the rotors, having a range of slopes between 10 and 12 dB increase in sound pressure level for an increase of .10 in C_T/σ.

Despite the discrepancies in absolute values the model data does reflect the sound pressure level changes due to operating conditions or rotor configuration with reasonable accuracy. Figure 31 for example compares the effects of reducing tip speed of the Model 347 rotor. From the above, it appears that models of isolated rotors in hover may be useful for sensitivity studies and possibly for comparing configurations, if not for full scale prediction. It would be desirable, however, to conduct additional studies to further verify the validity of using models for trend studies of noise generation of hovering rotors.

Tandem Rotors

Tandem rotor configurations can generate an impulsive noise signature due to interaction between the vortices shed by one rotor and the blades of the other. Figure 32a illustrates this phenomenon by smoke visualization on the Boeing Vertol Tandem Rotor Model (TRM) which was the source of model data for this study. The full scale data was from two modified versions of the CH-47 helicopter. The first (Figure 32b) had an aft pylon which had been increased in height by thirty inches but retained the three bladed rotor and thirty four percent overlap of the standard CH-47. The second aircraft was the Model 347 (Figure 32c) which retained the high pylon and had a one hundred and ten inch fuselage extension which reduced the overlap of its four bladed rotors to twenty-two percent.

The tandem rotor model, unfortunately, was limited to operating tip speeds of about 500 ft/secs. In order to account for this discrepancy use was made of in-house Boeing Vertol data which indicated that under conditions of constant blade-vortex separation, the sound pressure level varied approximately as the sixth order of the tip speed. These adjustments were made to the model data and are noted on the applicable figures.

The comparisons of model and full scale data are presented in Figures 33-36. The independent variable used is total cyclic trim. As the trim is increased both rotors tilt forward thereby decreasing the separation in the overlap region.

With the exception of the 34% overlap configuration at 120 knots the agreement between model and full scale data are all within 3 dB. No explanation for the discrepancy at 120 knots

is evident but careful examination of the data and trends tends to cast more suspicion on the full scale data than on the model data. Note that the relative ineffectiveness of cyclic trim at 40 knots and effectiveness at 80 knots displayed by the full scale data is well replicated by the model data. Examination of waveforms indicates that at the higher speeds of 120 and 128 knots the "N" wave associated with high advancing tip speed appears in both model and full scale data with the lower speed waveforms tending to display the higher frequency content pulse more characteristic of blade-vortex intersection.

The results of making a simple extension of the model to a non-overlapped configuration is compared with the 34% overlapped configuration in Figure 37. The 0% overlap data are singularly free of high frequency content which indicates complete freedom from an impulsive acoustical signature. It is investigations of this type, which would be prohibitively expensive in full scale, which make model testing extremely important to improving the basic understanding of rotor noise generation and reduction.

Main-Tail Rotor Interaction

During operation of the Model YUH-61 helicopter (Figure 38) as a tied down vehicle, or hovering in ground effect, an impulsive noise at main rotor blade passage period was noted directly behind the aircraft but greatly diminished to either side. During subsequent testing of a one fifth scale model (Figure 38a) acoustical measurements were made to further investigate this effect. Since the noise occurred at main rotor blade passage period, it was hypothesized that the source was interaction of the tail rotor with vortices shed from the main rotor blades.

Model and full scale data at three azimuth positions are compared in Figures 39a, b, c and show that the full scale situation was well reproduced by the model particularly with respect to the directivity of the noise and impulsiveness of the waveforms. Although, as noted, the tail rotor tip speed of the model was less than that of the full scale aircraft no analytical adjustment was made because the main rotor parameters were matched. The agreement of model and full scale data indicates that the impulsive noise generation is probably more strongly influenced by main rotor tip vortex strength than by tail rotor velocity.

Some interactive effects are presented in Figure 40. Most apparent is that the presence of the tail rotor increases the noise at main rotor passage period by approximately 5 dB, a value which would be considerably more difficult to obtain with a full scale aircraft than with a model because of the provisions which would be required to react the torque.

CONCLUSIONS AND RECOMMENDATIONS

Figure 41 summarizes the results of this study with respect to the accuracy with which small scale models can be used to predict peak-to-peak values of full scale data. The ordinate for each point represents the difference between an adjusted model data point and the value of the full scale data at the corresponding independent variable (if the model data falls between corresponding full scale data the value of the linear point to point interpolation is used). With the exception of the isolated rotor virtually all model data agreed with full scale data within six dB and the mean values within two dB. This is, in fact, no worse than agreements which are often experienced between repeat flights of full scale helicopters. Although the difference in absolute values for isolated rotors hovering in low winds have a greater disparity, the model data does display the same trends as the full scale data and can be used as an aid in selecting between rotor designs, if not to predict the absolute sound pressure levels.

The recommended measurement for evaluation is peak-to-peak sound pressure level although reasonable agreement can be achieved on a harmonic spectral basis. In making peak-to-peak measurements the pressure time histories should be inspected carefully to ensure that they reflect the expected type of rotor noise generating mechanism and also to determine whether averaging procedures should be used in the data reduction. In cases where the data contains transient pulses, and the maximum values are of interest, averaging techniques should not be used.

Testing in non-anechoic wind tunnels need not be a problem as long as reverberation and time delay calibrations of the type described in this report are employed.

It is recommended that the use of small scale models be encouraged for the studies of impulsive rotor noise due to high tip speed effects and to blade-vortex interactions in forward flight. The applicability to blade-vortex intersections in low speed descent should be investigated because this condition is of major importance in determining community noise exposure around heliports and is applicable to all helicopter configurations.

APPENDIX A

WIND TUNNEL MODEL DATA ADJUSTMENTS

TABLE A-1, DATA CORRECTIONS - ABSOLUTE HARMONIC SOUND PRESSURE LEVELS DERIVED FROM MODEL DATA - ISOLATED YUH-61A ROTOR (FIGURES 14 & 15)

HARMONIC NUMBER	MODEL DATA FREQUENCY Hz	(1) RAW DATA SPL dB	(2) DISTANCE ADJUSTMENT dB	ADJUSTED FOR DISTANCE dB	REVERBERATION ADJUSTMENT dB	ADJUSTED DATA dB	FULL SCALE DATA(3) SPL dB
1	92	116	-12	104	0	104	108
2	184	107		95	-5	90	100
3	276	105		93	-8	85	94
4	368	100		88	-7	81	91
5	460	101		89	-9	80	92
6	552	100		88	-9	79	91
7	644	100		88	-4	84	88
8	736	99		87	-6	81	89
9	828	99		87	-6	81	87
10	920	100		88	-5	83	84
11	1012	98		86	-5	81	80
12	1104	97		85	-5	80	79
13	1196	97		85	-6	79	78
14	1288	96		89	-6	78	76
15	1380	96		84	-6	78	75
16	1472	96		84	-6	78	73
17	1564	94		82	-6	76	73
18	1656	93		81	-6	75	73
19	1748	92		80	-6	74	76
20	1840	91		79	-4	75	78

(2) MODEL $D/d = \frac{10.36}{10.1} = 1.025$

FULL SCALE $D/d = \frac{206}{49} = 4.2$

$20 \text{ LOG } \frac{1.025}{4.2} = -12.2$ dB

(1) FIGURE 28C, $C_T/\sigma = .102$ (SPL = RELATIVE SPL + 60 dB)

(3) FIGURE 28C, $C_T/\sigma = .097$ (SPL = RELATIVE SPL + 50 dB)

TABLE A-2, DATA CORRECTIONS - ABSOLUTE HARMONIC SOUND PRESSURE LEVELS DERIVED FROM MODEL DATA - ISOLATED YUH-61A ROTOR (FIGURES 16 & 17)

HARMONIC NUMBER	FREQUENCY Hz	(1) RAW DATA SPL-dB	(2) TUNNEL VELOCITY ADJUSTMENT-dB	ADJUSTED FOR VELOCITY-dB	(3) DISTANCE ADJUSTMENT-dB	ADJUSTED FOR DISTANCE-dB	REVERBERATION ADJUSTMENT-dB	ADJUSTED DATA-dB	(4) FULL SCALE DATA-dB
1	58	118	0	118	-28 1	90	-10	80	90
2	117	132	0	132		104	-10	94	90
3	175	132	+ 1	133		105	-10	95	104
4	233	133	+ 5	138		110	-11	99	104
5	291	131	+ 7	138		110	- 8	102	94
6	350	131	+ 7	138		110	- 8	102	99
7	408	129	+ 8	137		109	-12	97	100
8	466	127	+10	137		109	-10	99	96
9	525	126	+10	136		108	-10	98	89
10	583	124	+ 4	128		100	-11	89	90
11	641	122	+ 4	126		98	-11	87	89
12	700	116	+ 4	120		92	-11	81	86
13	758	115	- 3	112		84	-10	74	78
14	816	124	- 3	121		93	-10	83	80
15	874	124	- 3	121		93	-10	83	82
16	933	117	-10	107		79	- 9	70	78
17	991	117	-10	107		79	- 9	70	70
18	1049	118	-10	108		80	- 9	71	78
19	1108	117	-10	107		79	- 9	70	78
20	1166	113	-10	103		75	-11	64	72

(1) FIGURE 23C M_T = 936 (SPL - RELATIVE SPL + 80 dB)

(2) INTERPOLATED FROM FIGURE 12

(3) MODEL D/d = $\frac{23\ 2}{16}$ = 1 45

FULL SCALE D/d = $\frac{2317}{60}$ = 38 6

20 LOG $\frac{1\ 45}{38\ 6}$ = -28 5 dB

(4) FIGURE 23C M_T = 935 (SPL = RELATIVE SPL = 50 dB)

MODEL

MACH NO. (M_T)	MEASURED DATA PEAK TO PEAK SPL, dB	DISTANCE CORRECTION ΔL dB	ADJUSTED FOR DISTANCE PEAK TO PEAK SPL, dB	WIND TUNNEL VELOCITY CORRECTION ΔV dB (REF.FIG. 13)	ADJUSTED FOR DISTANCE & TUNN. VEL. PEAK TO PEAK SPL, dB
.728	114	-28.5	85.5	3	88.5
.793	118		89.5	3	92.5
.840	122.5		94	3.5	97.5
.856	123		94.5	3.5	98
.872	125.5		97	3.5	100.5
.889	126.5		98	3.5	101.5
.905	130		101.5	4	105.5
.920	135		106.5	4	110.5
.936	136.5		108	4	112
.952	137.5		109	4	113
.969	140		111.5	4	115.5
.985	142		113.5	4	117.5

TABLE A-3
ADJUSTMENTS - PEAK TO PEAK DATA - FIGURE 23A

MODEL

MACH NO. (M_T)	MEASURED DATA PEAK TO PEAK SPL, dB	DISTANCE CORRECTION ΔL dB	ADJUSTED FOR DISTANCE PEAK TO PEAK SPL, dB	WIND TUNNEL VELOCITY CORRECTION ΔV dB (REF.FIG. 13)	ADJUSTED FOR DISTANCE & TUNN. VEL. PEAK TO PEAK SPL, dB
.807	121	-28.5	92.5	3.5	96
.835	123		94.5	3.5	98
.864	127		98.5	3.5	102
.897	133		104.5	4	108.5
.922	136.5		108	4	112
.950	143.0		114.5	4	118.5
.980	146.5		118	4	122

TABLE A-4
ADJUSTMENTS - PEAK TO PEAK DATA - FIGURE 24A

MODEL

MACH NO. (M_T)	MEASURED DATA PEAK TO PEAK SPL, dB	DISTANCE CORRECTION ΔL dB	ADJUSTED FOR DISTANCE PEAK TO PEAK SPL, dB	WIND TUNNEL VELOCITY CORRECTION ΔV dB (REF.FIG. 13)	ADJUSTED FOR DISTANCE & TUNN. VEL. PEAK TO PEAK SPL, db
.689	109.5	-25.5	84	2.5	86.5
.770	116		90.5	2.5	93
.798	120.5		95	2.5	97.5
.828	127		101.5	3	104.5
.893	131		105.5	3	108.5
.915	132.5		107	3	110
.942	137		111.5	3.5	115
.970	140		114.5	3.5	118

TABLE A-5
ADJUSTMENTS - PEAK TO PEAK DATA - FIGURE 25A

MODEL

C_T/σ	MEASURED DATA PEAK TO PEAK SPL, dB	DISTANCE CORRECTION ΔL dB	ADJUSTED FOR DISTANCE PEAK TO PEAK SPL, dB
.015	117.5	-12	105.5
.028	117.5		105.5
.046	119		107
.064	120.5		108.5
.084	123		111
.102	127		115
.120	128		116
.127	129.5		117.5

TABLE A-6
ADJUSTMENTS - PEAK TO PEAK DATA - FIGURE 28A

MODEL

C_T/σ	MEASURED DATA PEAK TO PEAK SPL, dB	DISTANCE CORRECTION ΔL dB	ADJUSTED FOR DISTANCE PEAK TO PEAK SPL, dB
.040	114	-4.5	109.5
.060	120.5		116
.080	119.5		115
.090	121.5		117
.100	122		117.5
.110	123		118.5
.120	125		120.5
.130	125		120.5

TABLE A-7
ADJUSTMENTS - PEAK TO PEAK DATA - FIGURE 29A

MODEL

C_T/σ	MEASURED DATA PEAK TO PEAK SPL, dB	DISTANCE CORRECTION ΔL dB	ADJUSTED FOR DISTANCE PEAK TO PEAK SPL, dB	ΔV_T CORRECTION 60 LOG $\frac{751}{726}$ FT/SEC (FULL SCALE) FT/SEC (MODEL) dB	ADJUSTED FOR DISTANCE & V_T SPL, dB
.031	108	2.5	110.5	1	111.5
.050	110.5	↓	113	↓	114
.070	113	↓	115.5	↓	116.5
.092	113.5	↓	116	↓	117
.100	115	↓	117.5	↓	118.5
.110	117	↓	119.5	↓	120.5
.120	118.5	↓	121	↓	122
.130	121	↓	123.5	↓	124.5
.140	121	↓	123.5	↓	124.5

TABLE A-8
ADJUSTMENTS - PEAK TO PEAK DATA - FIGURE 30A

TABLE A-9

ADJUSTMENTS - PEAK TO PEAK DATA - FIGURE 33A, 34A, 35A

MODEL

	TOTAL TRIM,DEG	MEASURED DATA PEAK TO PEAK SPL, dB	DISTANCE CORRECTION ΔL dB	ADJUSTED FOR DISTANCE PEAK TO PEAK SPL, dB	TUNNEL VELOCITY CORRECTION ΔV dB (REF.FIG.13)	ΔV_T CORRECTION 60 LOG $\frac{722 \text{ FT/SEC}}{500 \text{ FT/SEC}}$ dB	ADJUSTED FOR DISTANCE, TUNN. VEL. & ΔV_T PEAK TO PEAK SPL, dB
40 KTS	0	108.5	-8	100.5	1	9.5	111
	6.0	110.5		102.5			113
	9.0	111		103			113.5
80 KTS	0	104.5		96.5	1.5		107.5
	6.0	107.5		99.5			110.5
	9.0	109.5		101.5			112.5
120 KTS	0	103.5		95.5	2.5		107.5
	9.0	106		98			110

MODEL

	TOTAL TRIM,DEG	MEASURED DATA PEAK TO PEAK SPL, dB	DISTANCE CORRECTION ΔL dB	ADJUSTED FOR DISTANCE PEAK TO PEAK SPL, dB	TUNNEL VELOCITY CORRECTION ΔV dB (REF.FIG. 13)	Δ V_T CORRECTION 60 LOG $\frac{738}{450}$ FT/SEC FT/SEC dB	ADJUSTED FOR DISTANCE, TUNN. VEL. & Δ V_T PEAK TO PEAK SPL, dB
131 KTS	13.4	108	-14.5	93.5	1.5	13	108
	15.8	109	-14.5	94.5	1.5	13	109

TABLE A-10
ADJUSTMENTS - PEAK TO PEAK DATA - FIGURE 36A

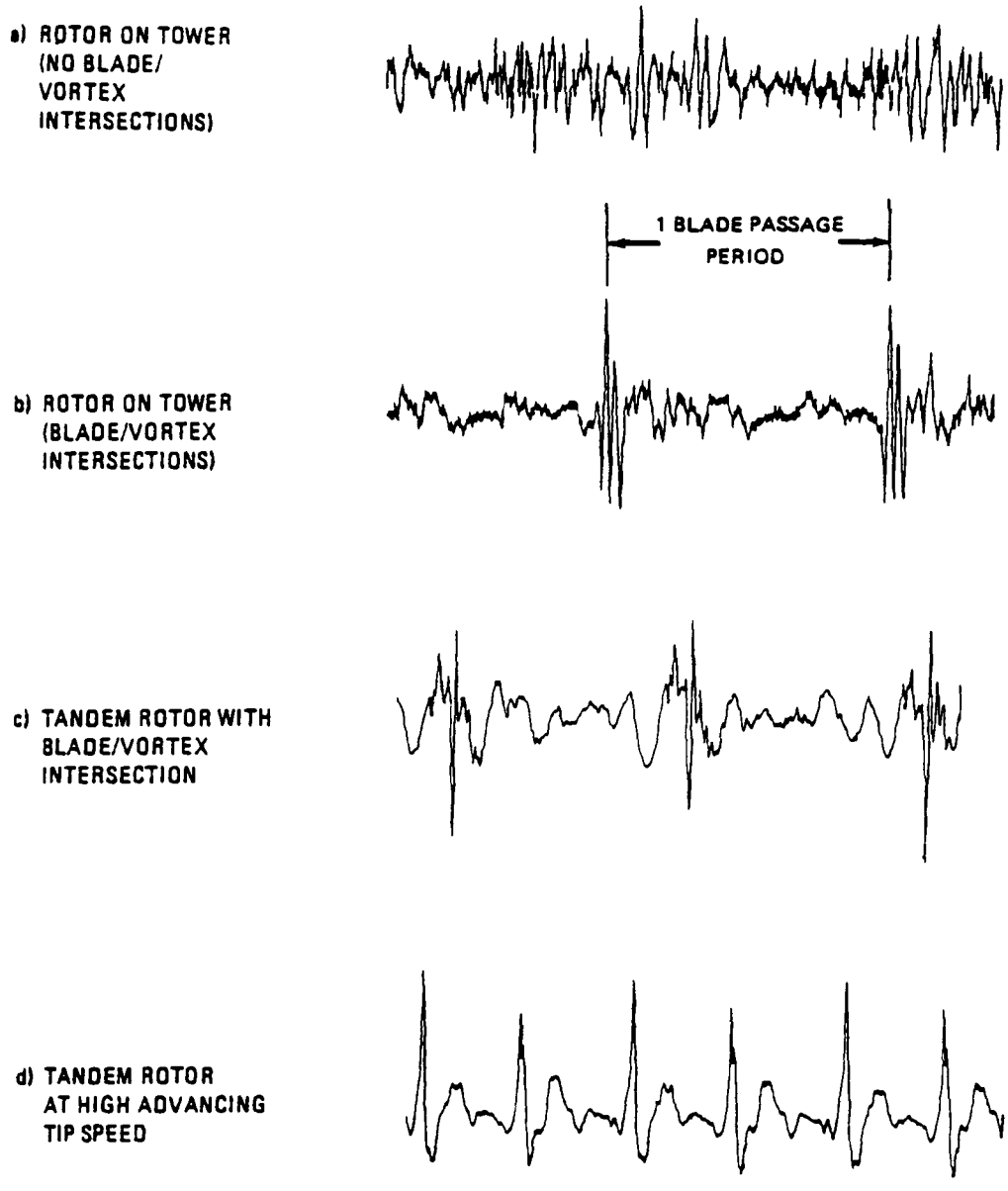

Figure 1 - Helicopter Noise Signatures in the Time Domain

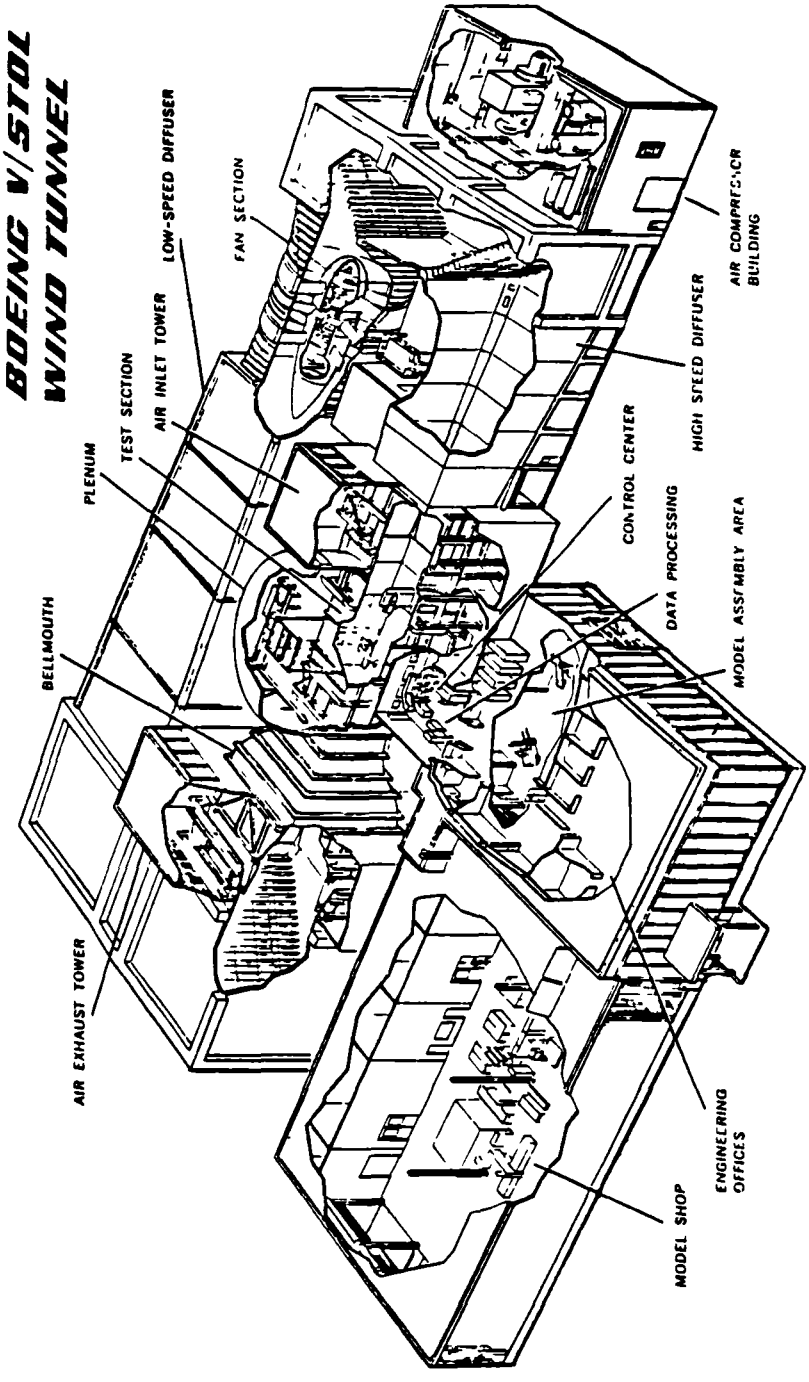

Figure 2 - Boeing Vertol V/STOL Wind Tunnel

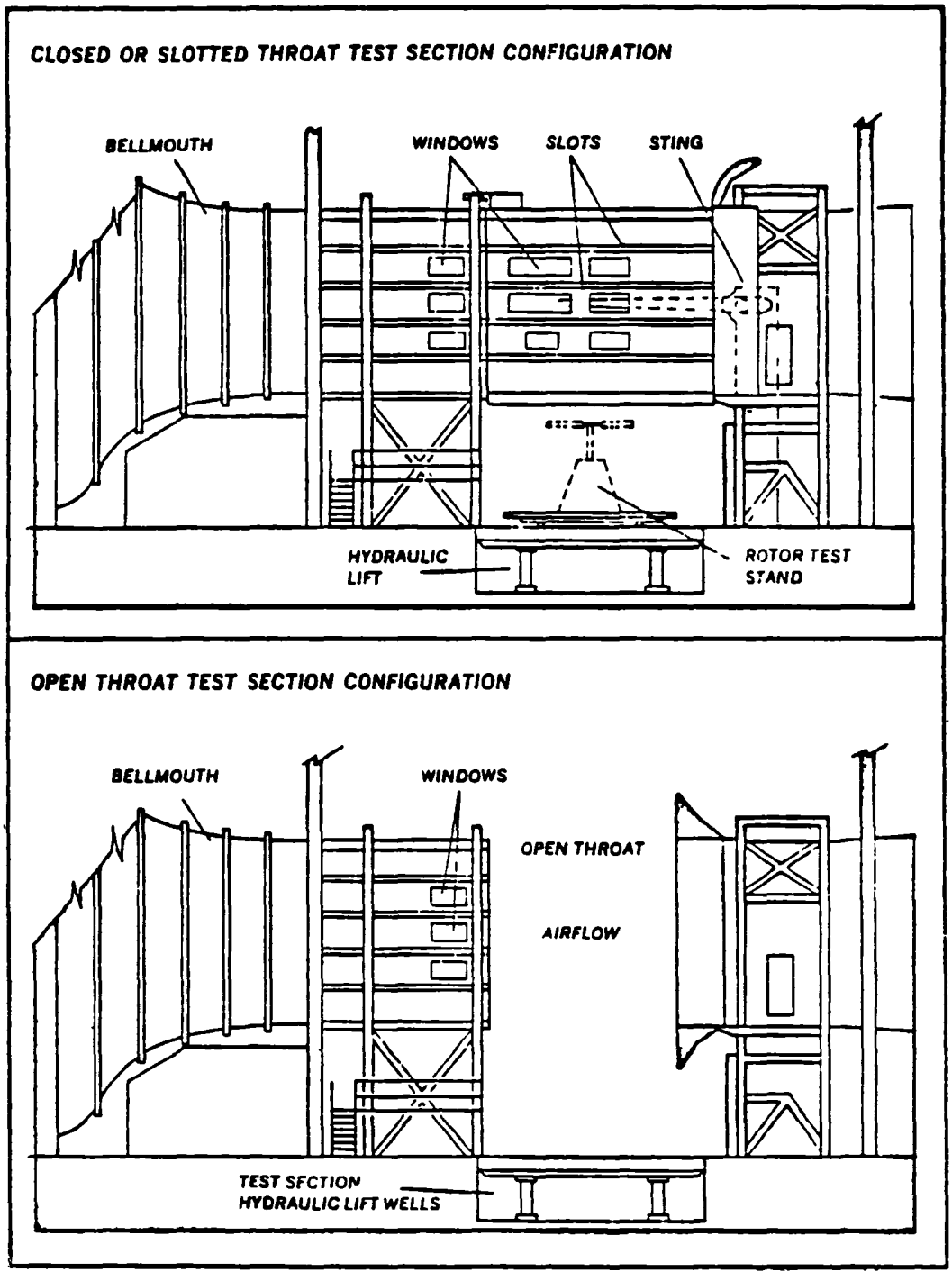

Figure 3 - Wind Tunnel Configurations

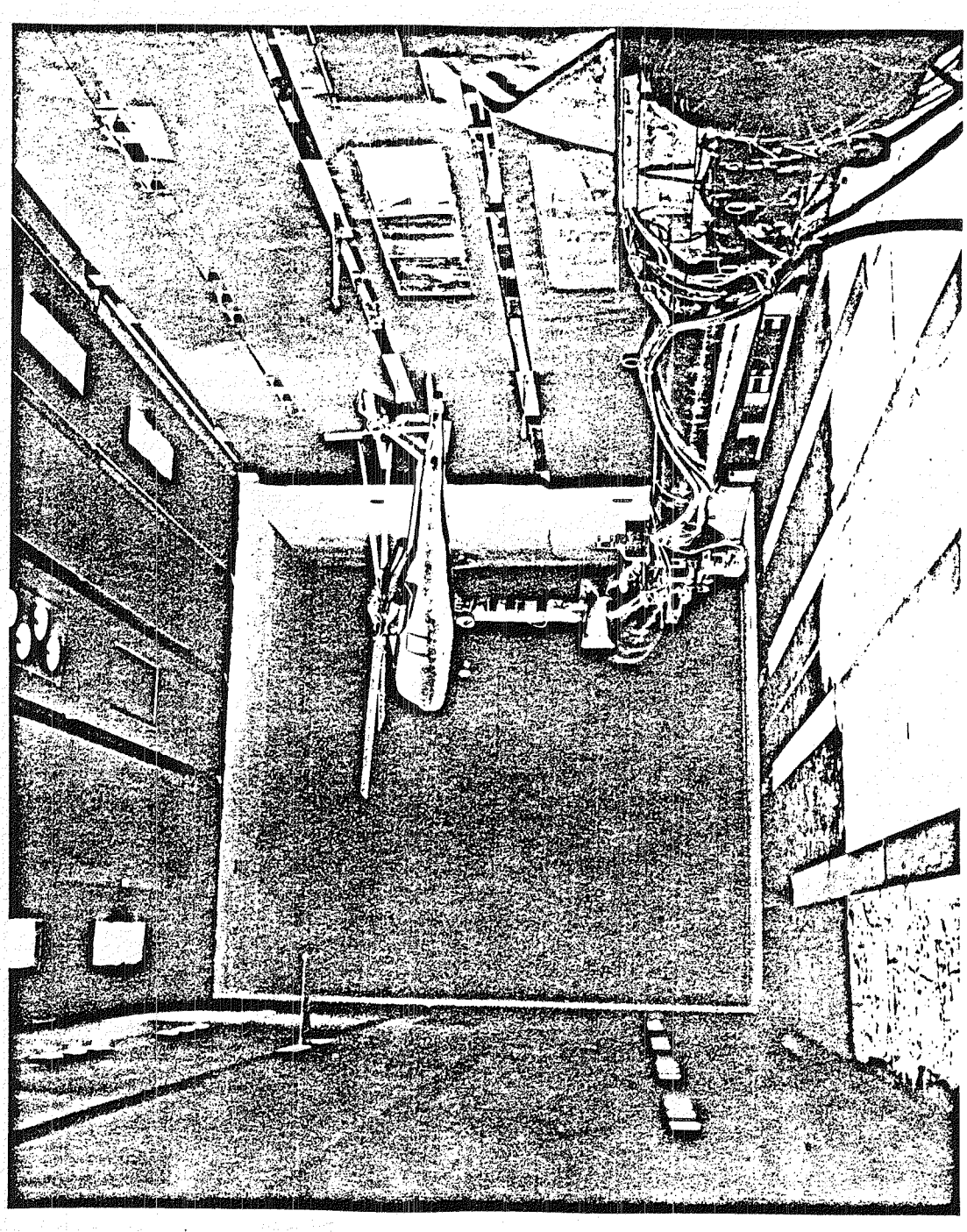

Figure 4 - Typical Wind Tunnel Installation

Figure 5 - Effect of Averaging on Wind Tunnel Data

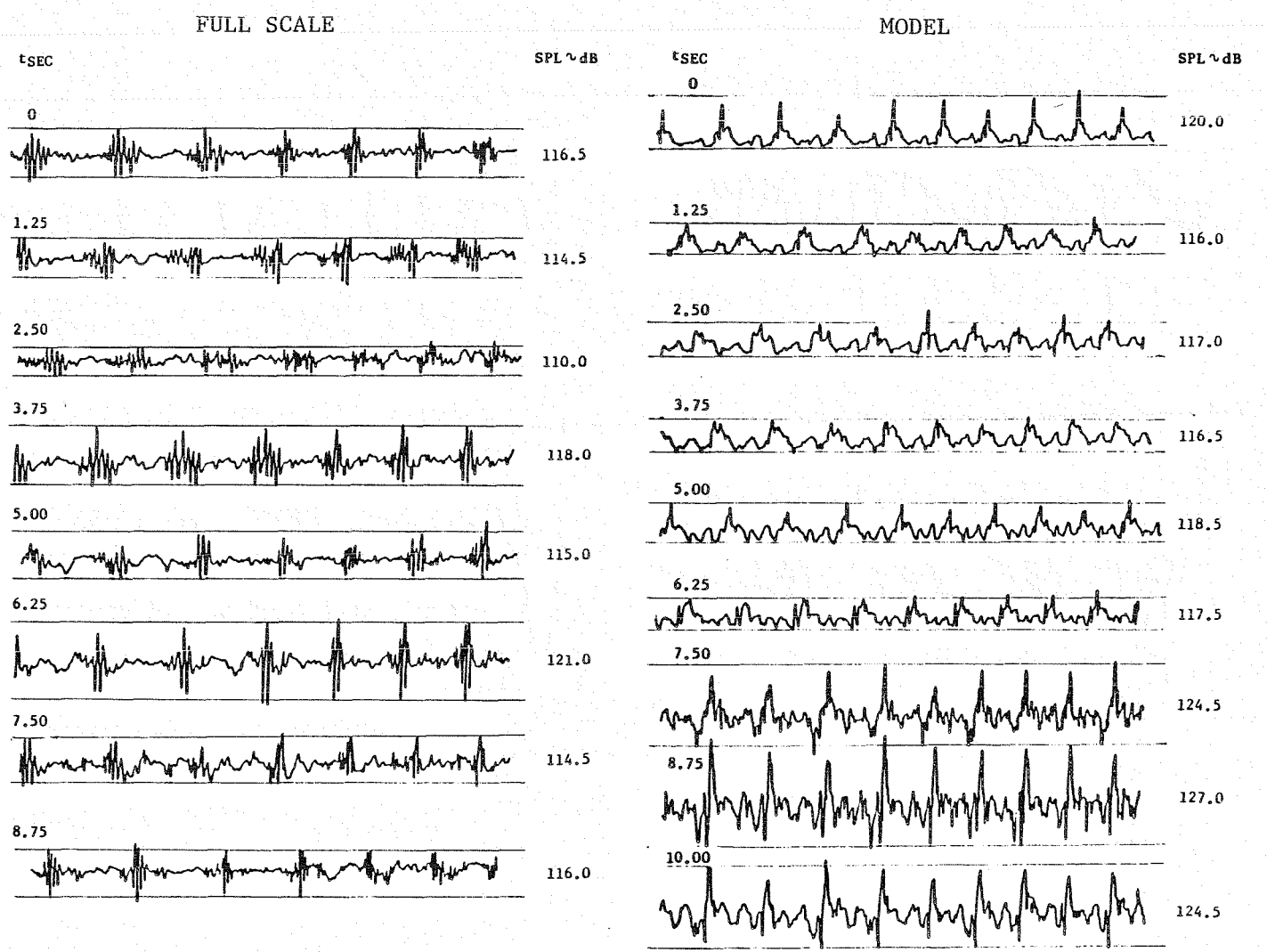

Figure 6 - Scatter of Test Data

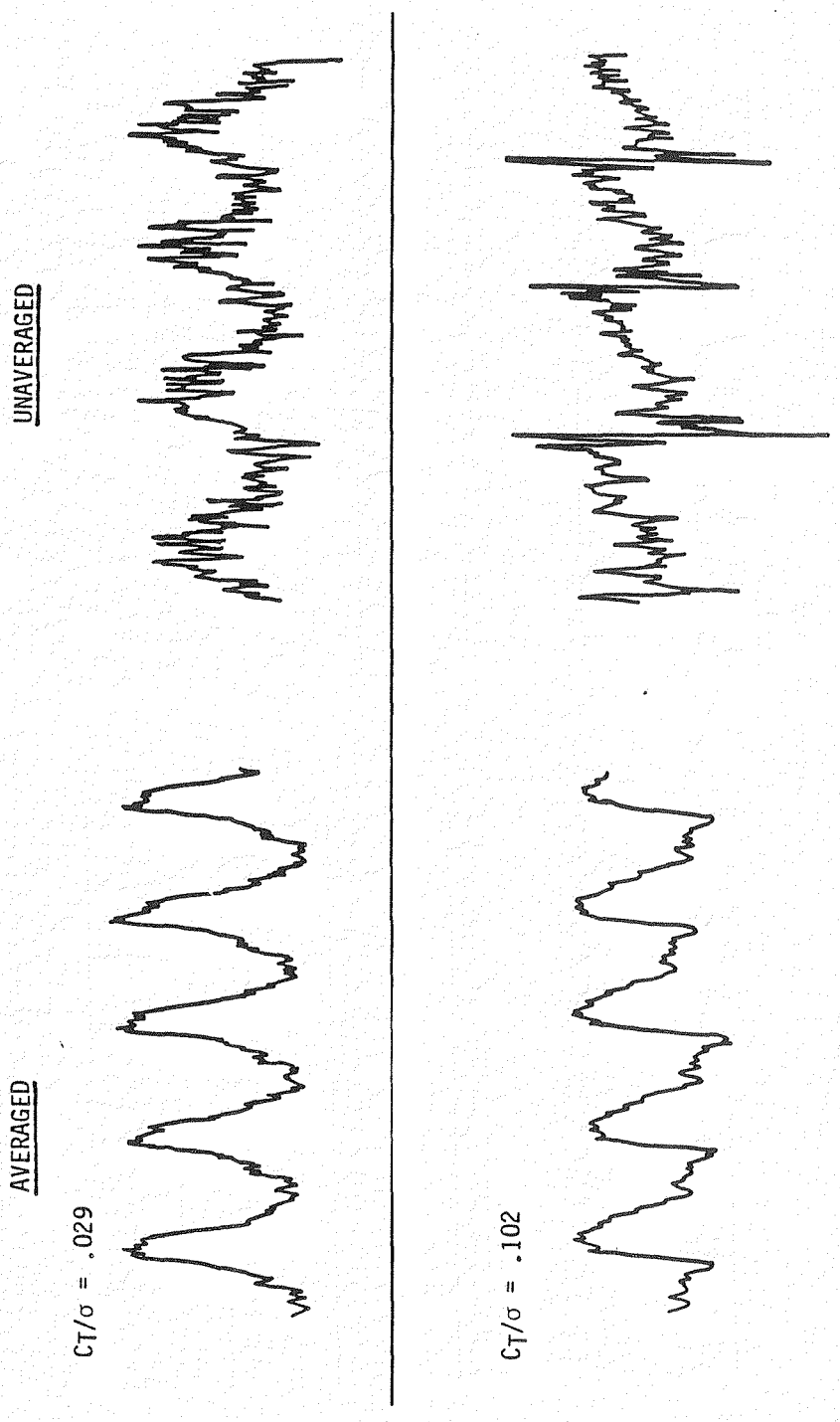

Figure 7 - Effect of Time Averaging on Transient Data

MODEL

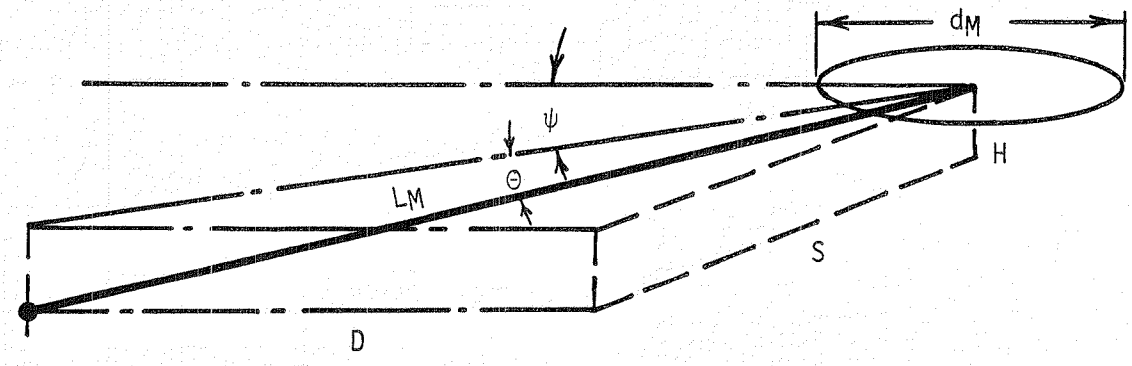

RANGE OF PARAMETERS

	H/d	S/d	D/d
MODEL	.1-.6	0-1.5	1.0-3.6
FULL SCALE	.5-9.2	0-4.1	.6-38

FULL SCALE

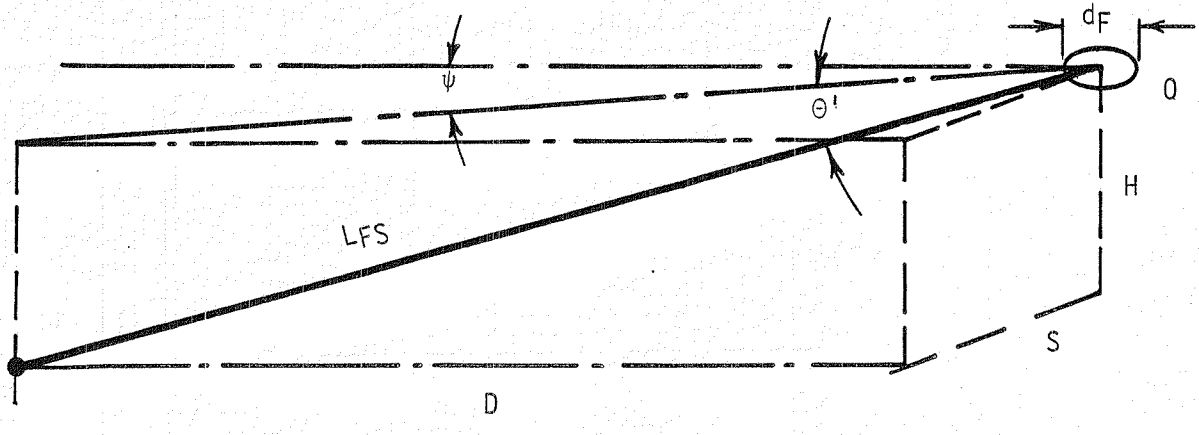

SELECT FULL SCALE DATA WHEN AIRCRAFT DISTANCE IS SUCH THAT $\Theta \approx \Theta'$.

$$\Delta L = 20 \text{ LOG } \frac{L_M/d_M}{L_{FS}/d_{FS}}$$

FIGURE 8. MICROPHONE-ROTOR GEOMETRIC RELATIONSHIPS

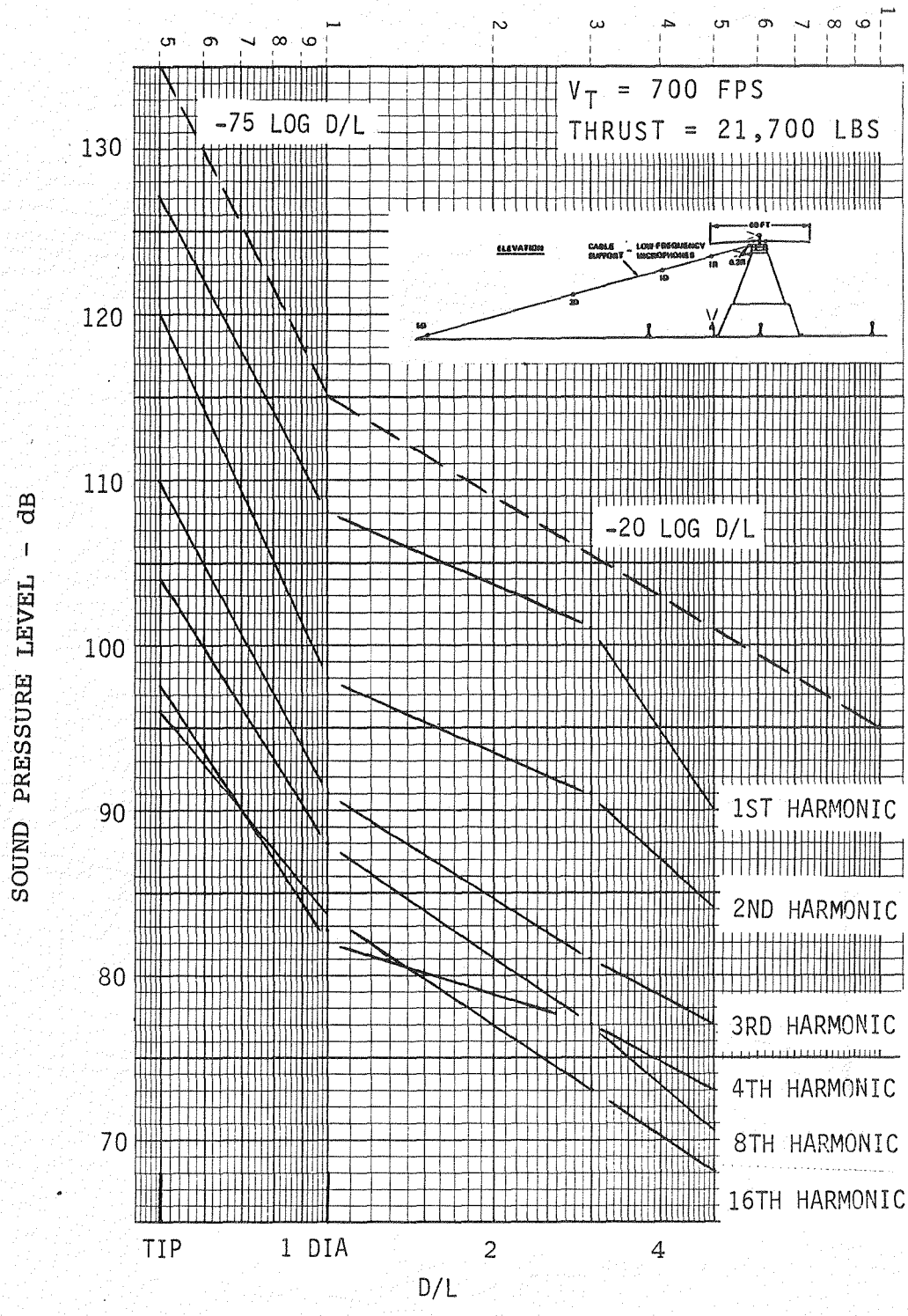

FIGURE 9. ROTOR TOWER NOISE PROPAGATION

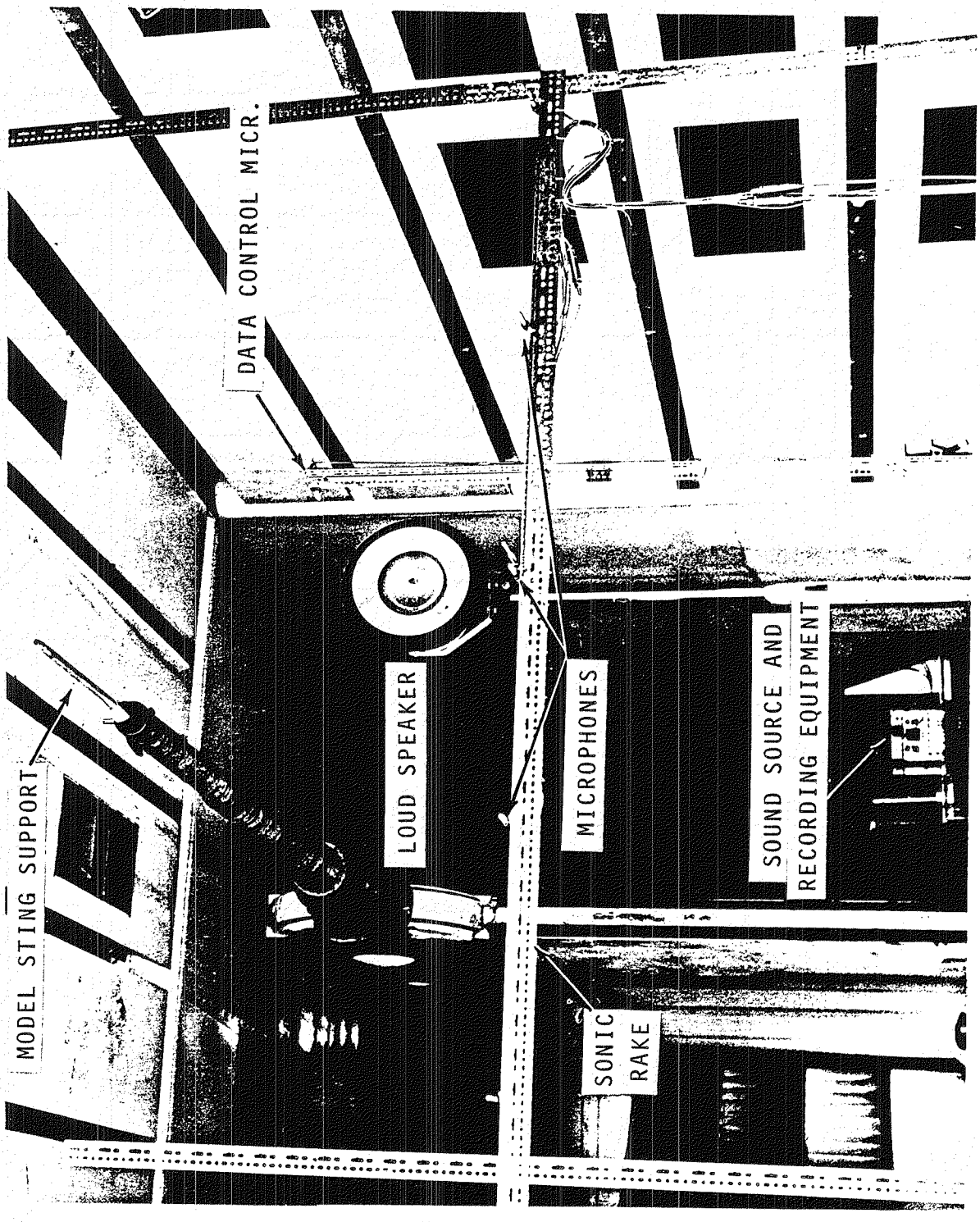

FIGURE 10. WIND TUNNEL ACOUSTICAL CALIBRATION
(TEST SECTION LOOKING DOWNWIND)

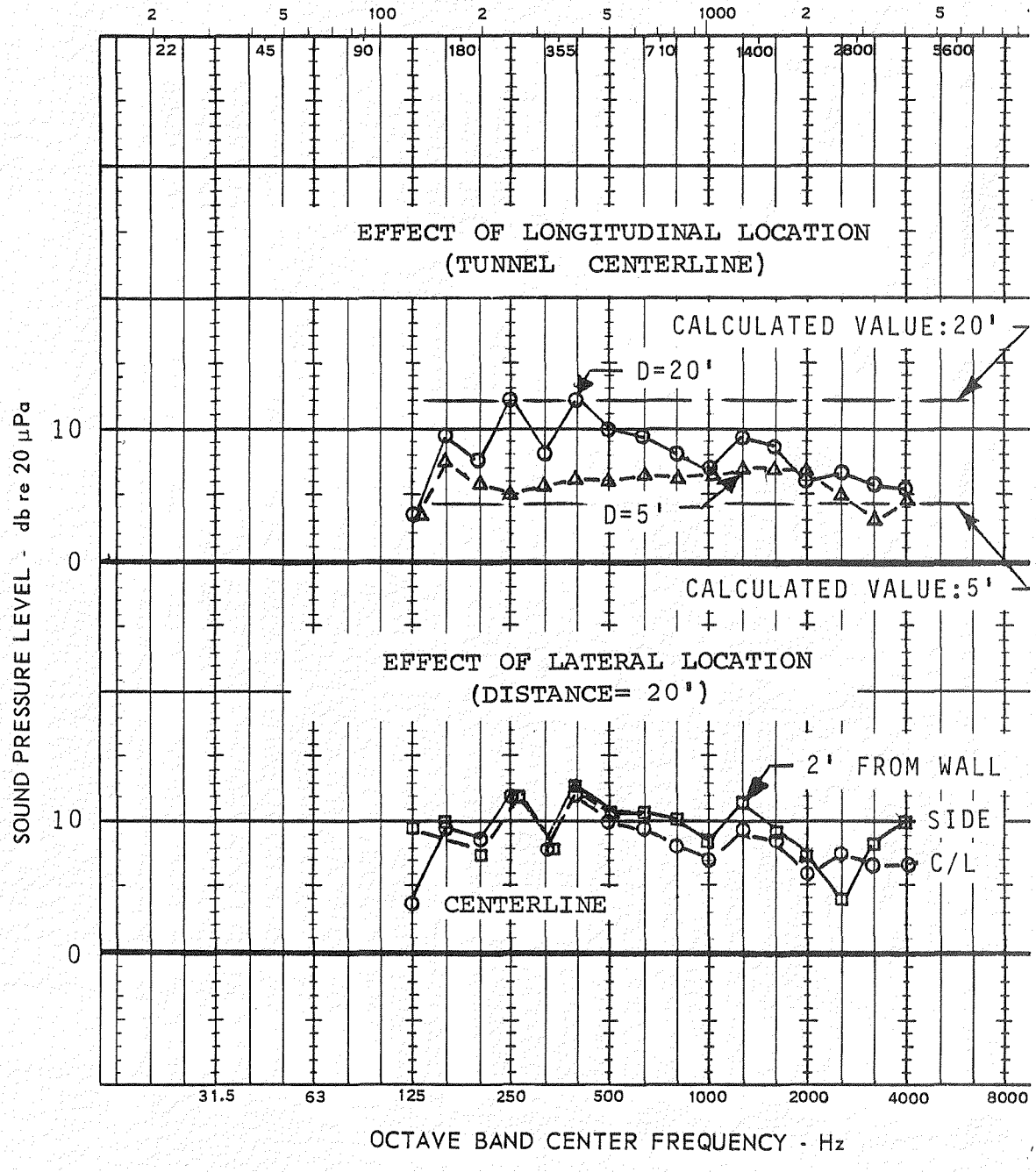

FIGURE 11. WIND TUNNEL REVERBERATION CORRECTION(PURE TONES)

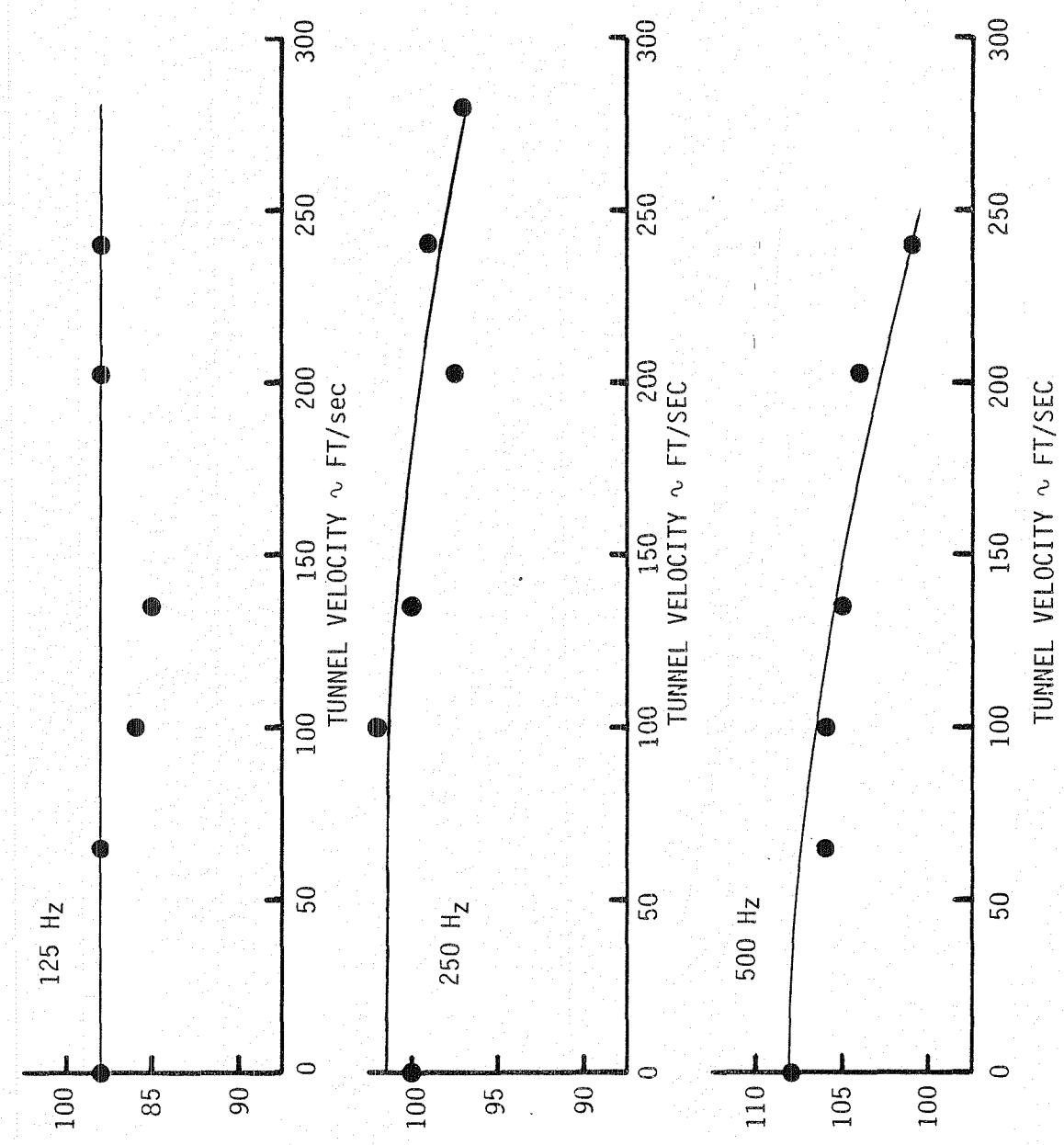

FIGURE 12A. EFFECT OF WIND TUNNEL VELOCITY ON SPL,MICROPHONE NO. 3, 20 FT UPSTREAM & 8 FT SIDELINE (WALL STING) 125,250,500 H_z @ 1/3-OCTAVE BAND FREQUENCY

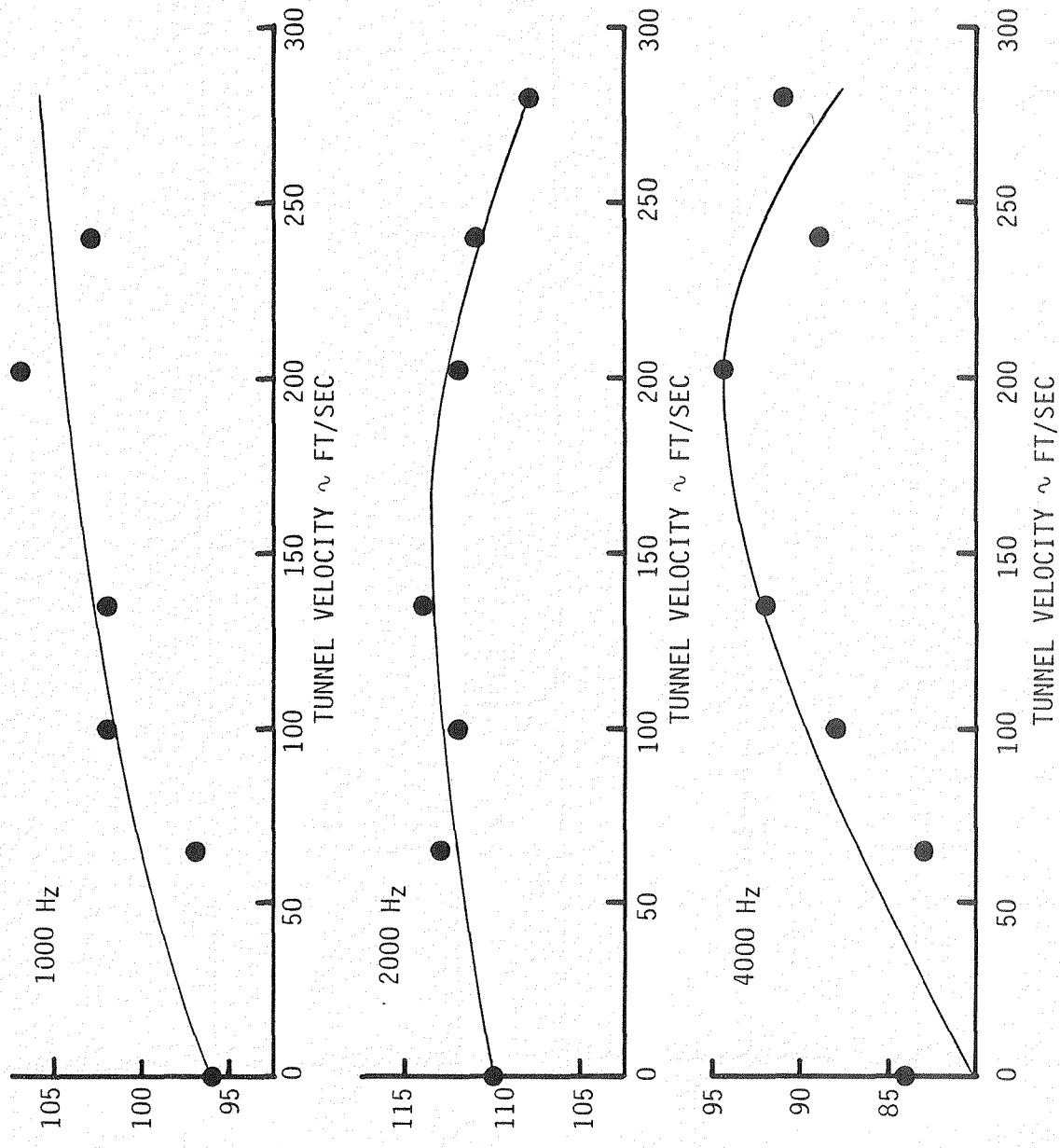

FIGURE 12B. EFFECT OF WIND TUNNEL VELOCITY ON SPL,MICROPHONE NO. 3, 20 FT UPSTREAM & 8 FT SIDELINE (WALL STING) 1000,2000,4000 H_z @ 1/3-OCTAVE BAND FREQUENCY

FIGURE 13. CALIBRATION OF WIND TUNNEL SPL-dB, ROTOR NOISE/SPEAKER SOURCE

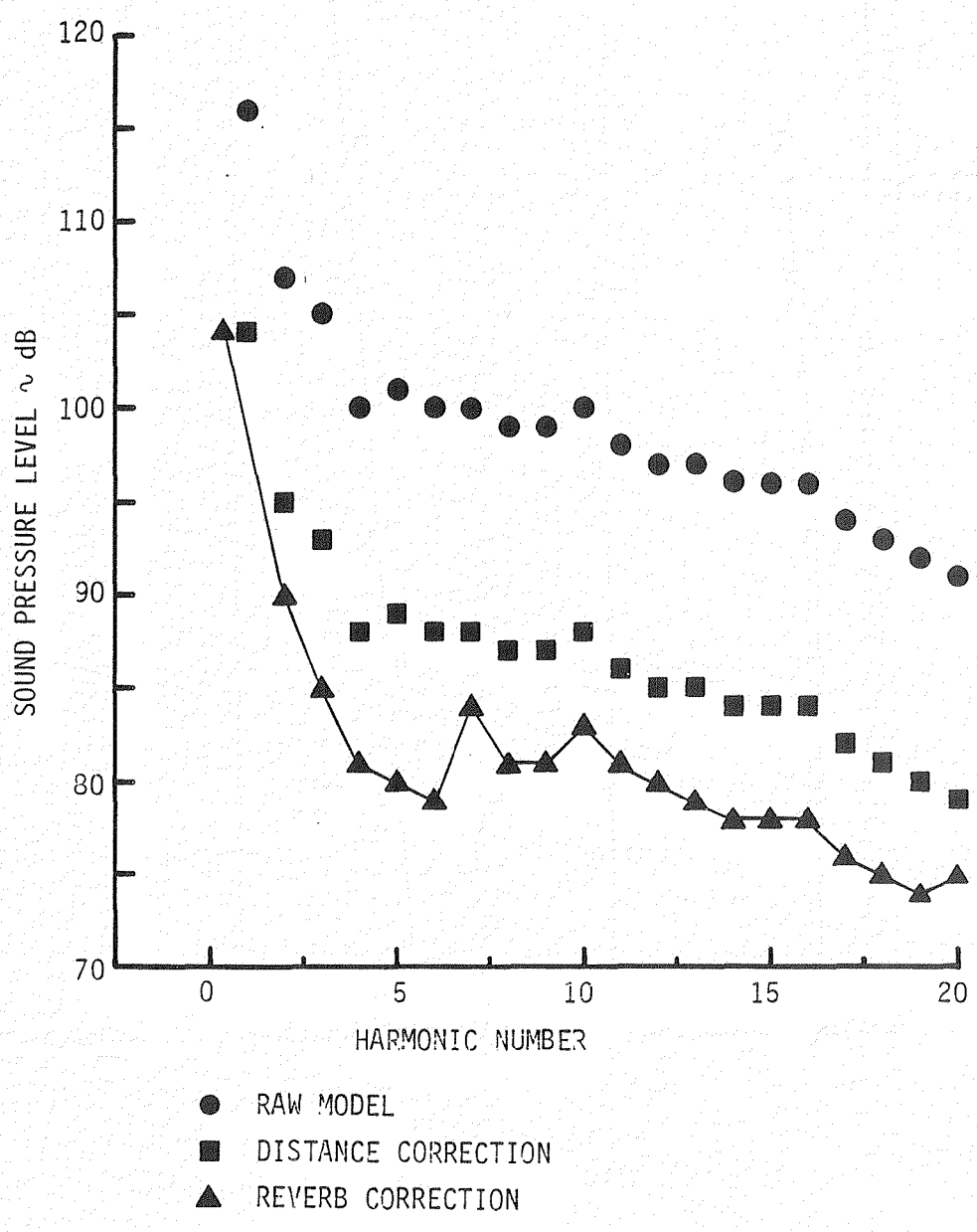

FIGURE 14. ABSOLUTE HARMONIC SOUND PRESSURE LEVELS DERIVED FROM MODEL DATA-ISOLATED YUH-61A ROTOR

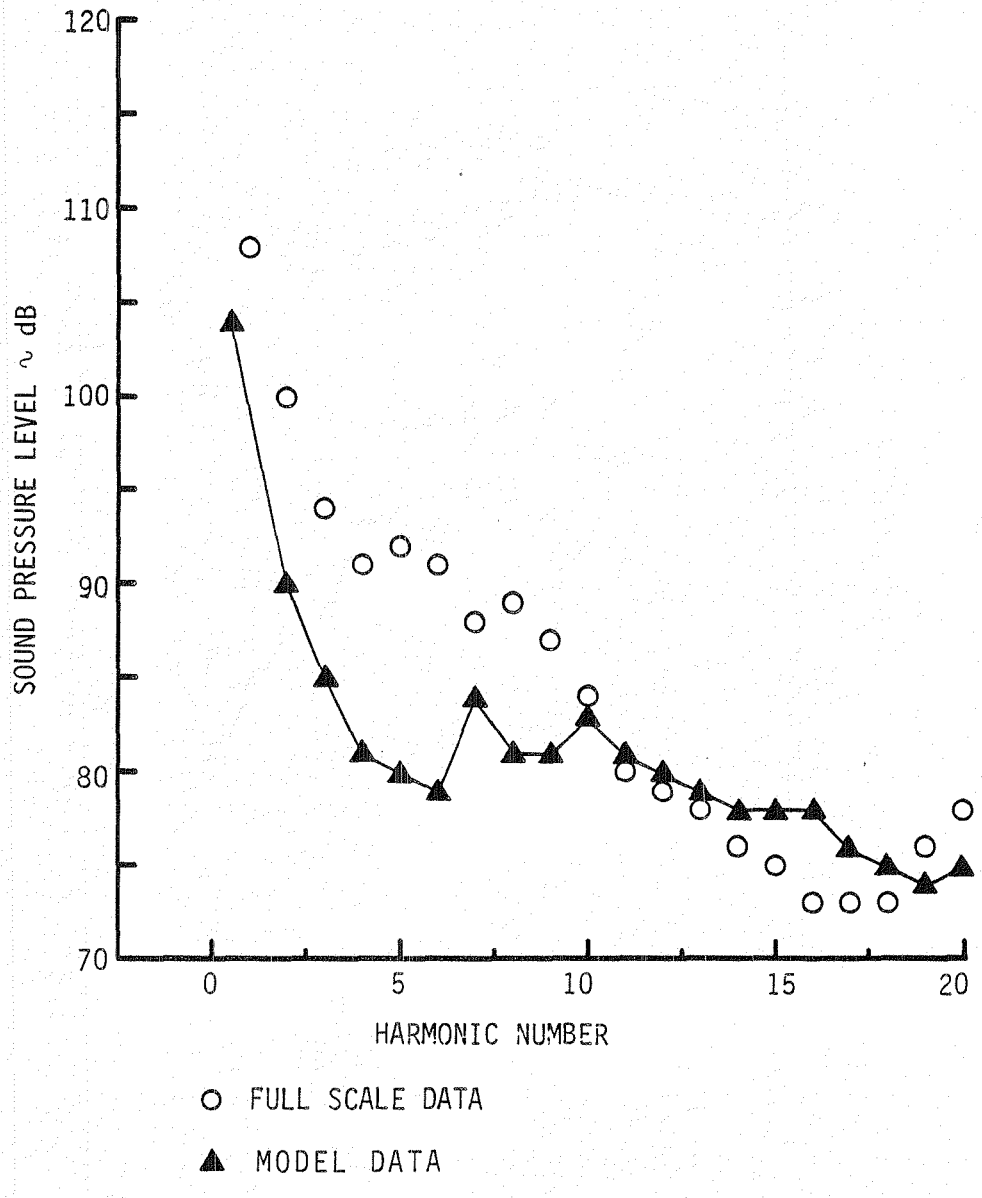

FIGURE 15. COMPARISON OF ABSOLUTE HARMONIC SOUND PRESSURE LEVELS DERIVED FROM MODEL AND FULL SCALE DATA-ISOLATED YUH-61A ROTOR

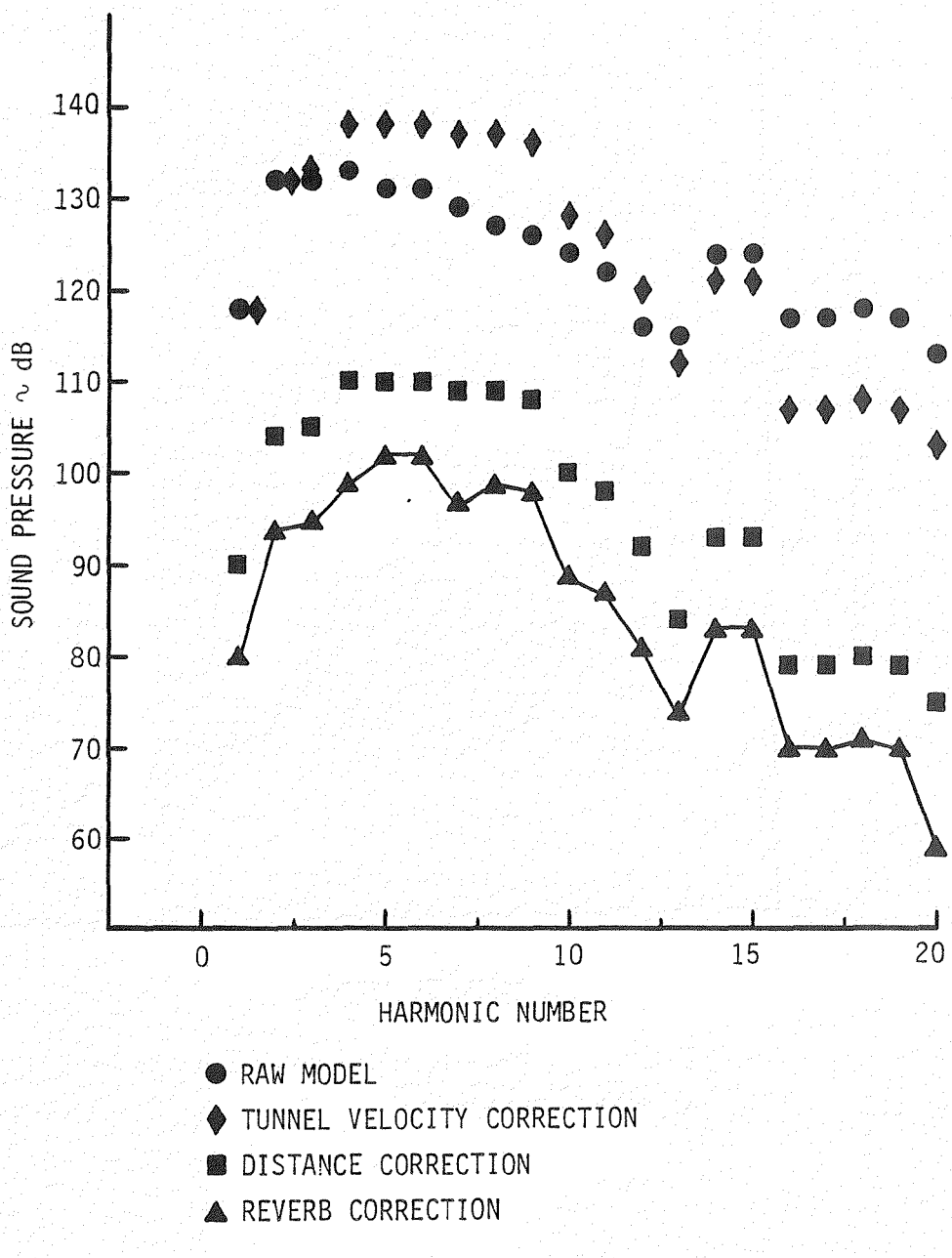

FIGURE 16. ABSOLUTE HARMONIC SOUND PRESSURE LEVELS DERIVED FROM MODEL DATA-FORWARD FLIGHT MODEL 347 ROTOR

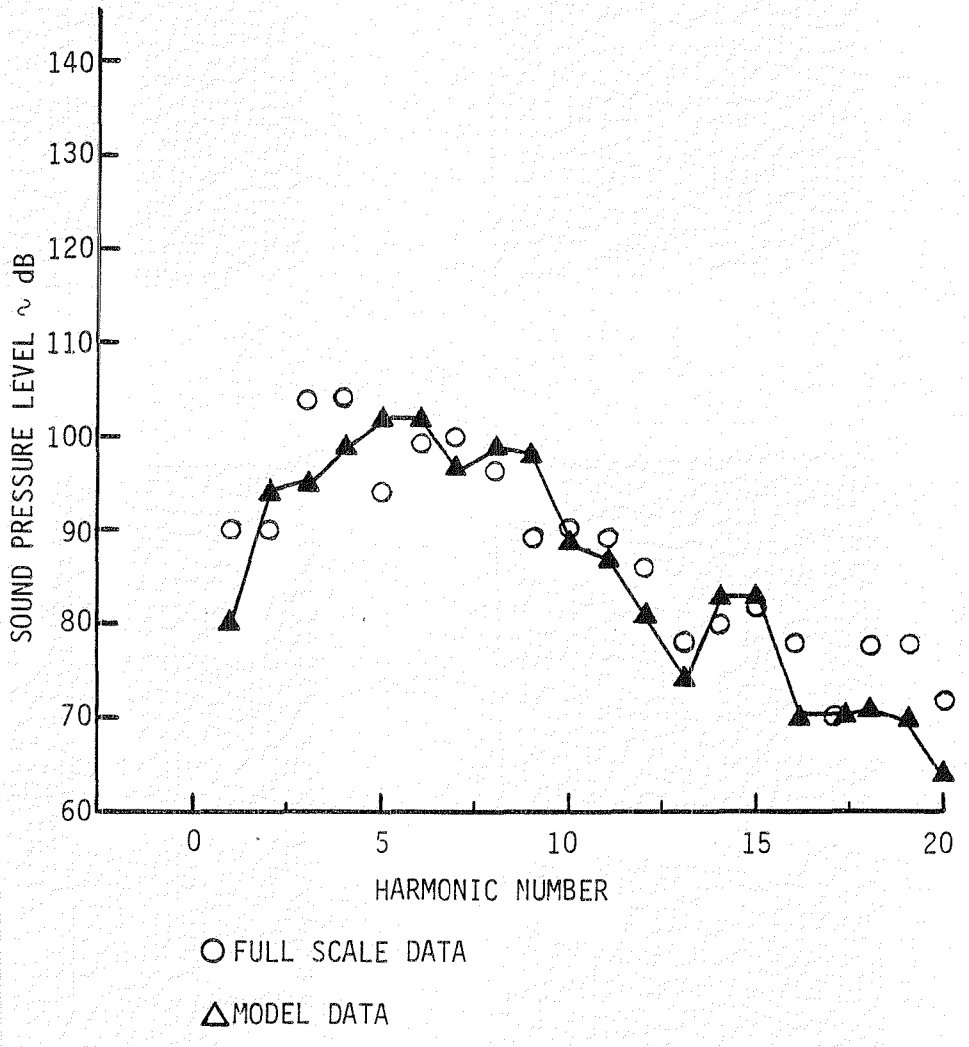

FIGURE 17. COMPARISON OF ABSOLUTE HARMONIC SOUND PRESSURE LEVELS DERIVED FROM MODEL AND FULL SCALE DATA-FORWARD FLIGHT, MODEL 347 ROTOR

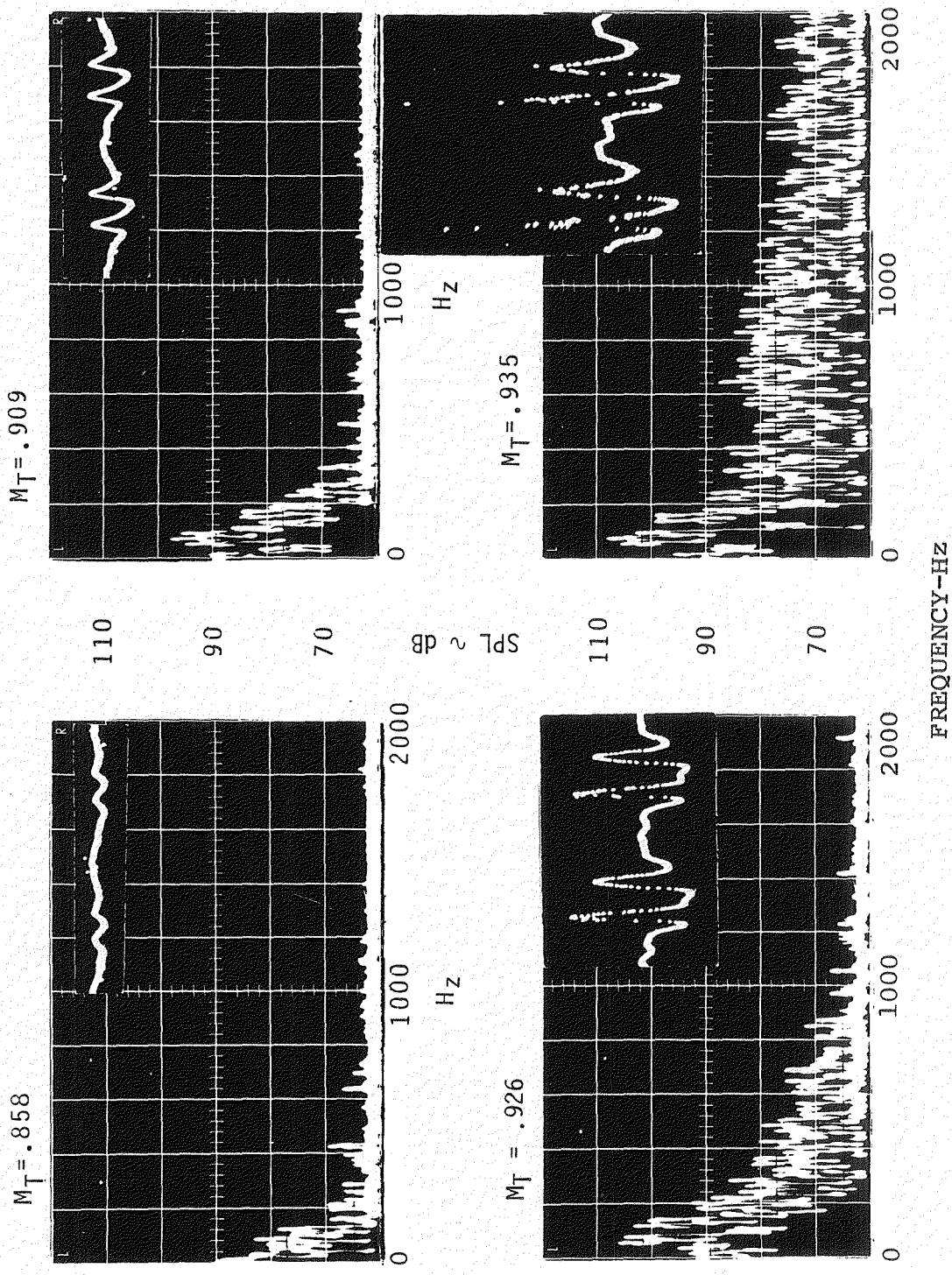

FIGURE 18. ADVANCING TIP MACH NUMBER EFFECT-WAVEFORMS AND SPECTRA

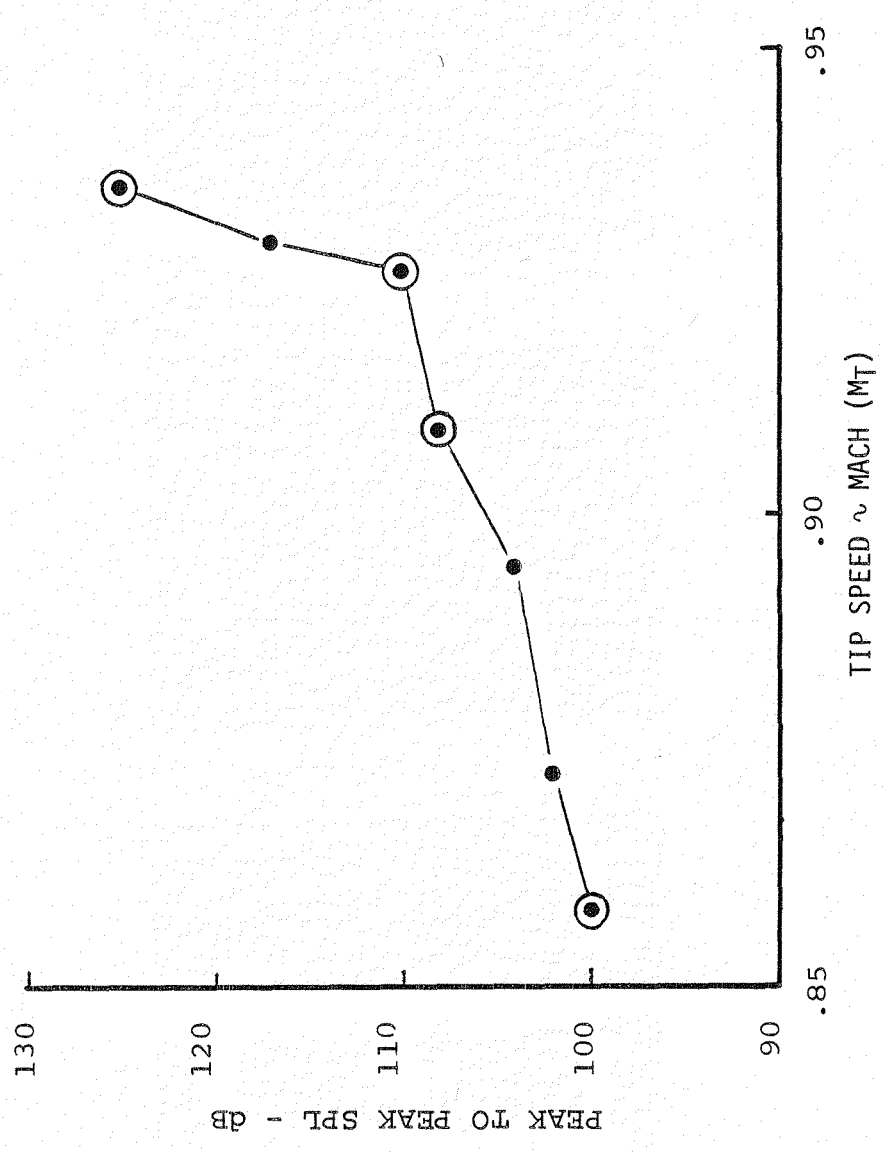

FIGURE 19. ADVANCING TIP MACH NUMBER EFFECT-AMPLITUDE

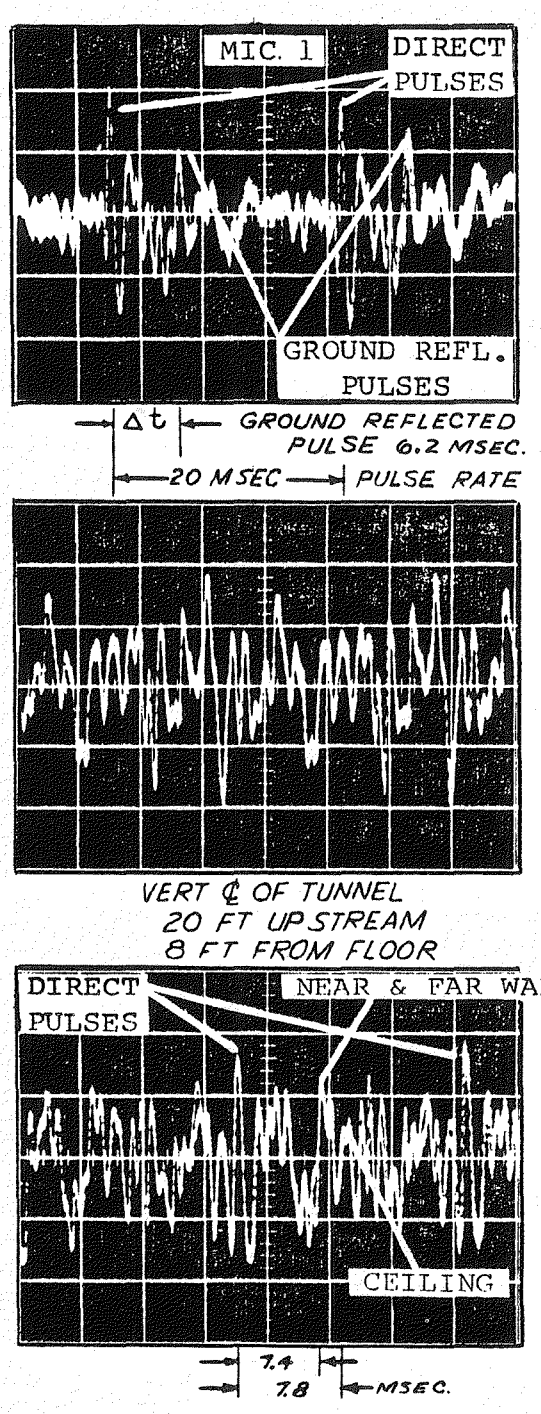

FREE FIELD

SLOTS OPEN

SLOTS CLOSED

FIGURE 20. COMPARISONS OF FREE-FIELD AND REVERBERENT TUNNEL TEST SECTION BOUNDARIES ON THE WAVEFORM OF AN IMPULSIVE MODEL ROTOR

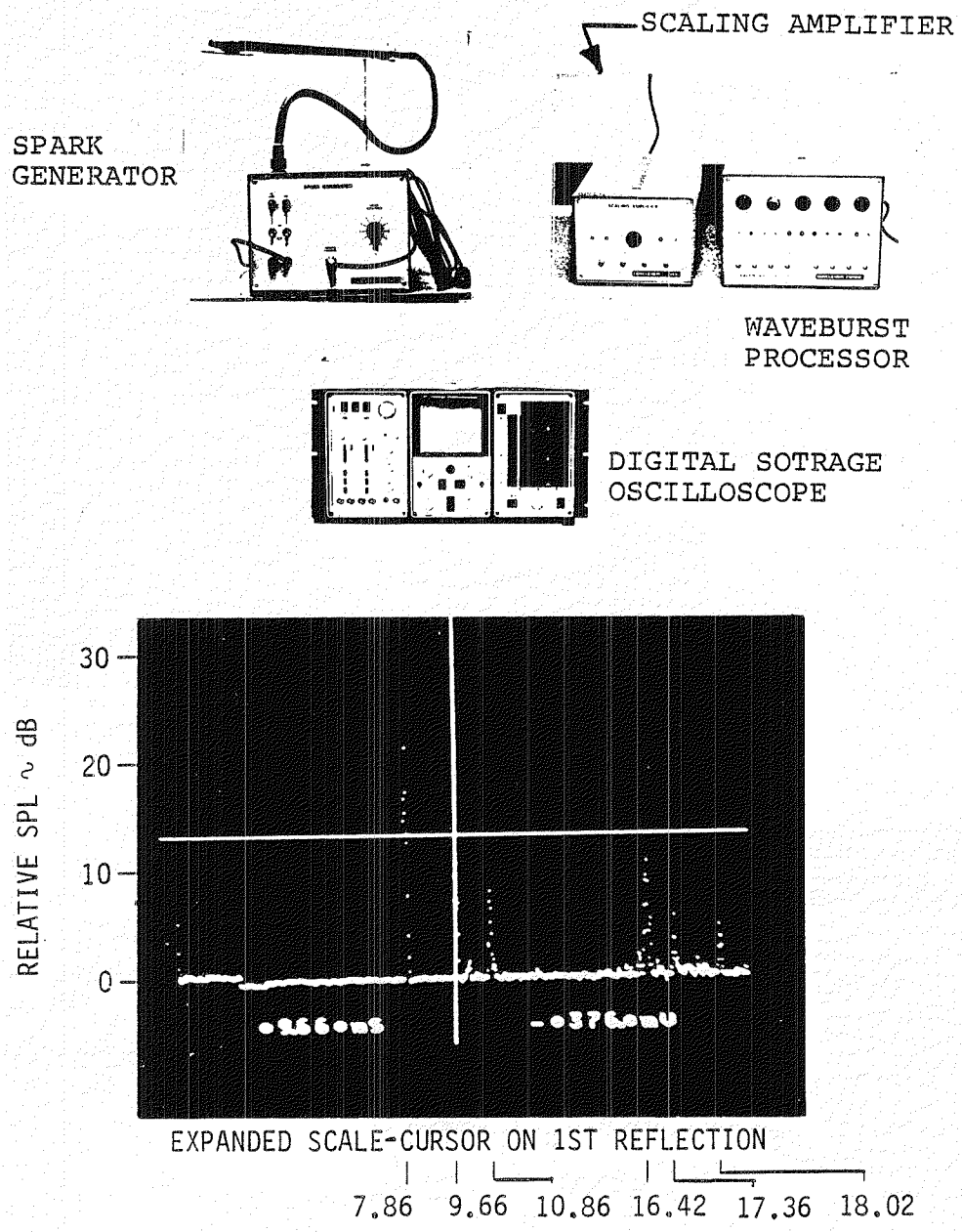

FIGURE 21. TYPICAL RESULTS OF WIND TUNNEL REVERBERATION TEST

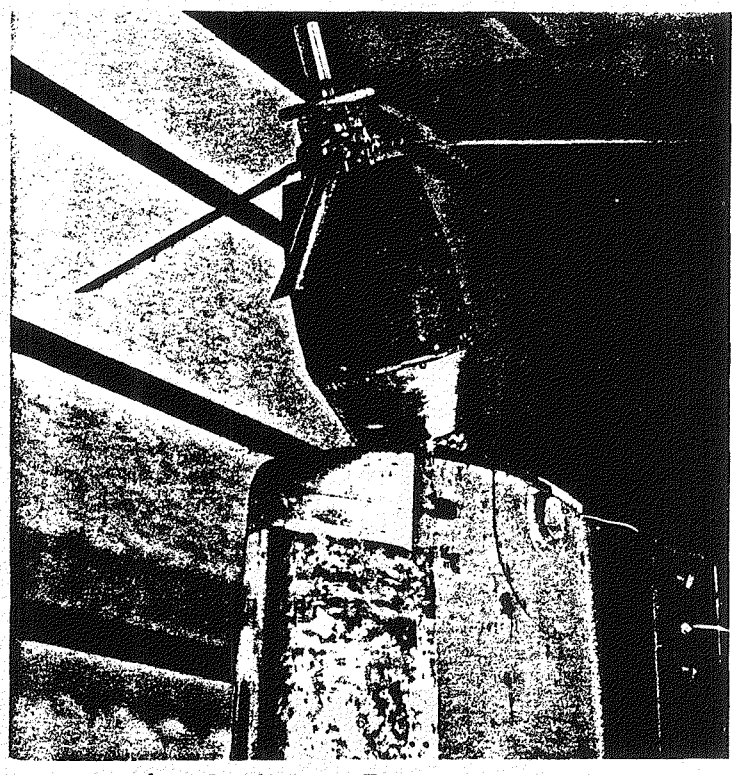

A. DYNAMIC ROTOR TEST STAND

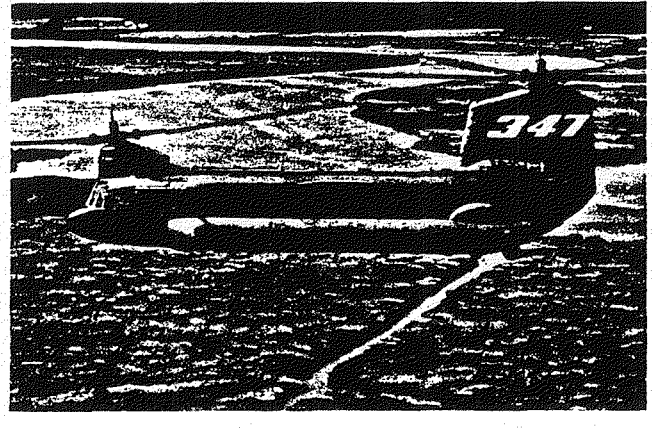

B. MODEL 347

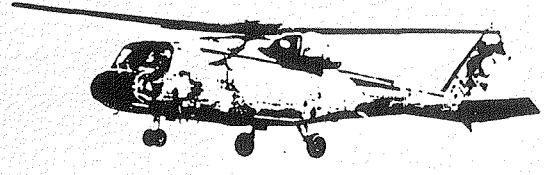

C. YUH-61A

FIGURE 22. TEST ARTICLES - TIP SPEED EFFECTS

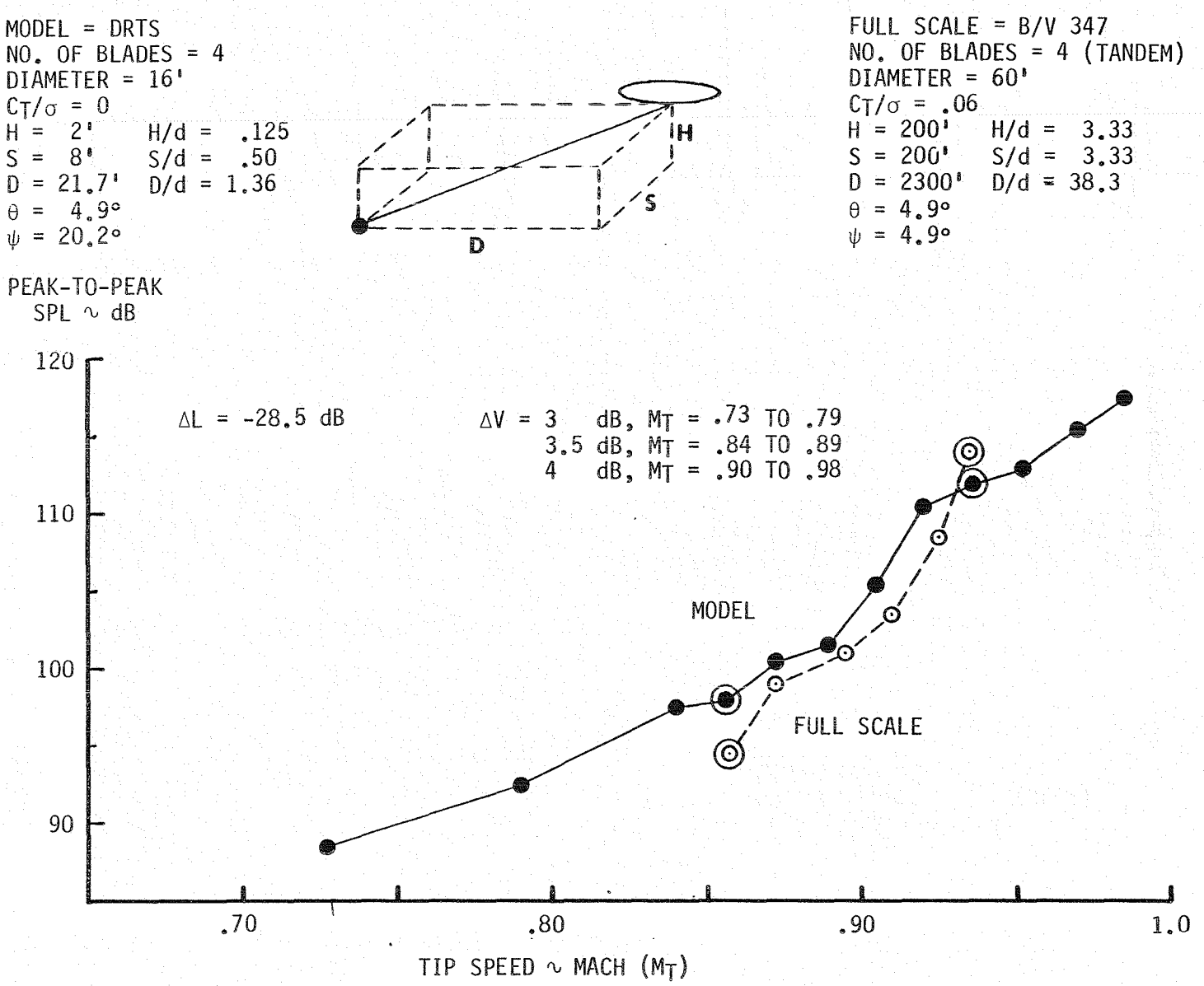

FIGURE 23A. COMPARISON OF MODEL AND FULL SCALE DATA - TIP SPEED EFFECTS - CH-47C ROTOR WITH 6% TIP THICKNESS - AMPLITUDE

FIGURE 23B. COMPARISON OF MODEL AND FULL SCALE DATA - TIP SPEED EFFECTS - CH-47C ROTOR WITH 6% TIP THICKNESS - WAVEFORMS

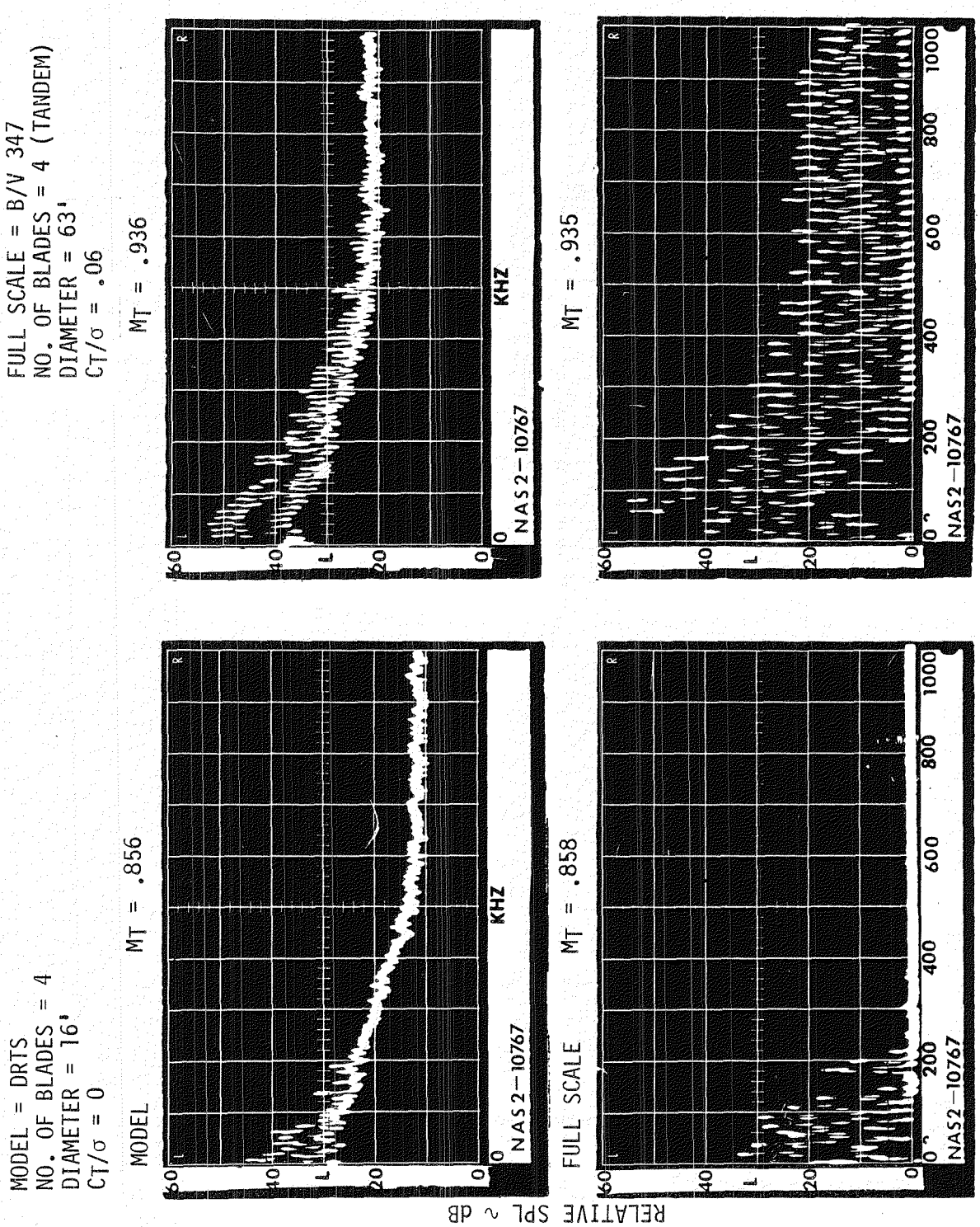

FIGURE 23C. COMPARISON OF MODEL AND FULL SCALE DATA - TIP SPEED EFFECTS - CH-47C ROTOR WITH 6% TIP THICKNESS - SPECTRA

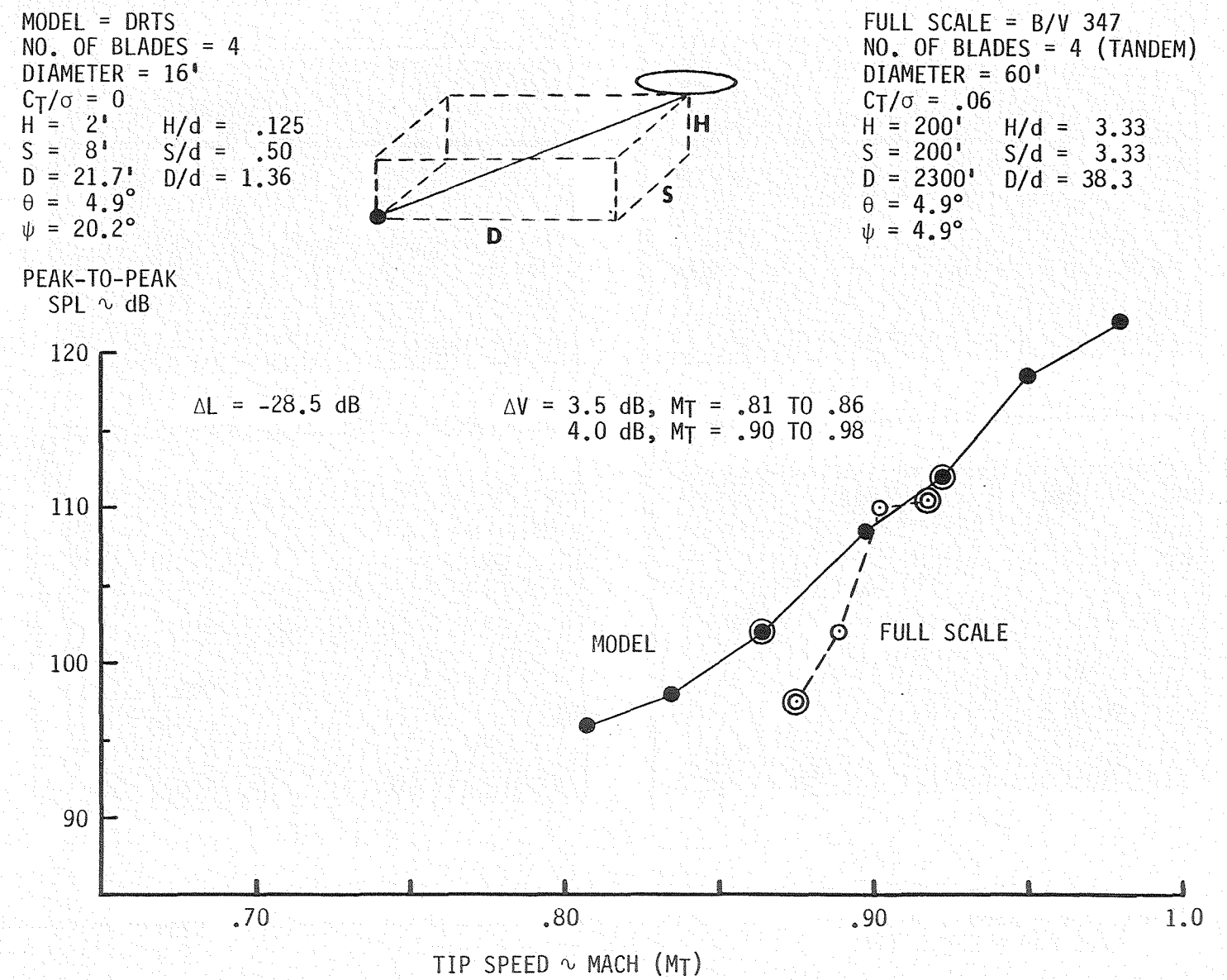

FIGURE 24A. COMPARISON OF MODEL AND FULL SCALE DATA - TIP SPEED EFFECTS - CH-47C ROTOR WITH 10% TIP THICKNESS - AMPLITUDE

FIGURE 24B. COMPARISON OF MODEL AND FULL SCALE DATA - TIP SPEED EFFECTS - CH-47C ROTOR WITH 10% TIP THICKNESS - WAVEFORMS

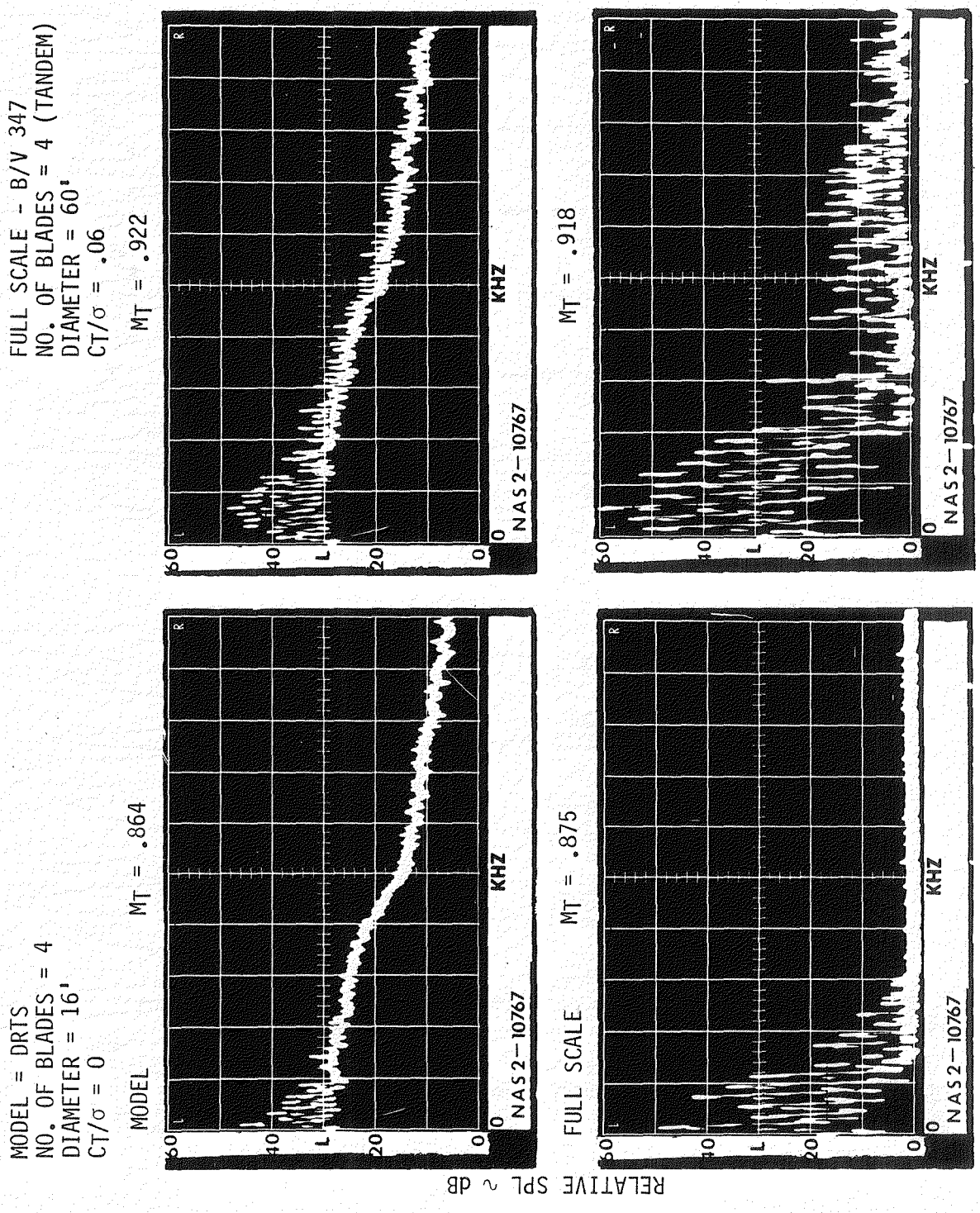

FIGURE 24C. COMPARISON OF MODEL AND FULL SCALE DATA - TIP SPEED EFFECTS - CH-47C ROTOR WITH 10% TIP THICKNESS - SPECTRA

FIGURE 25A. COMPARISON OF MODEL AND FULL SCALE DATA - TIP SPEED EFFECTS - YUH-61A - ROTOR

FIGURE 25B. COMPARISON OF MODEL AND FULL SCALE DATA - TIP SPEED EFFECTS - YUH-61A - WAVEFORMS

FIGURE 25c. COMPARISON OF MODEL AND FULL SCALE DATA - TIP SPEED EFFECTS - YUH-61A - SPECTRA

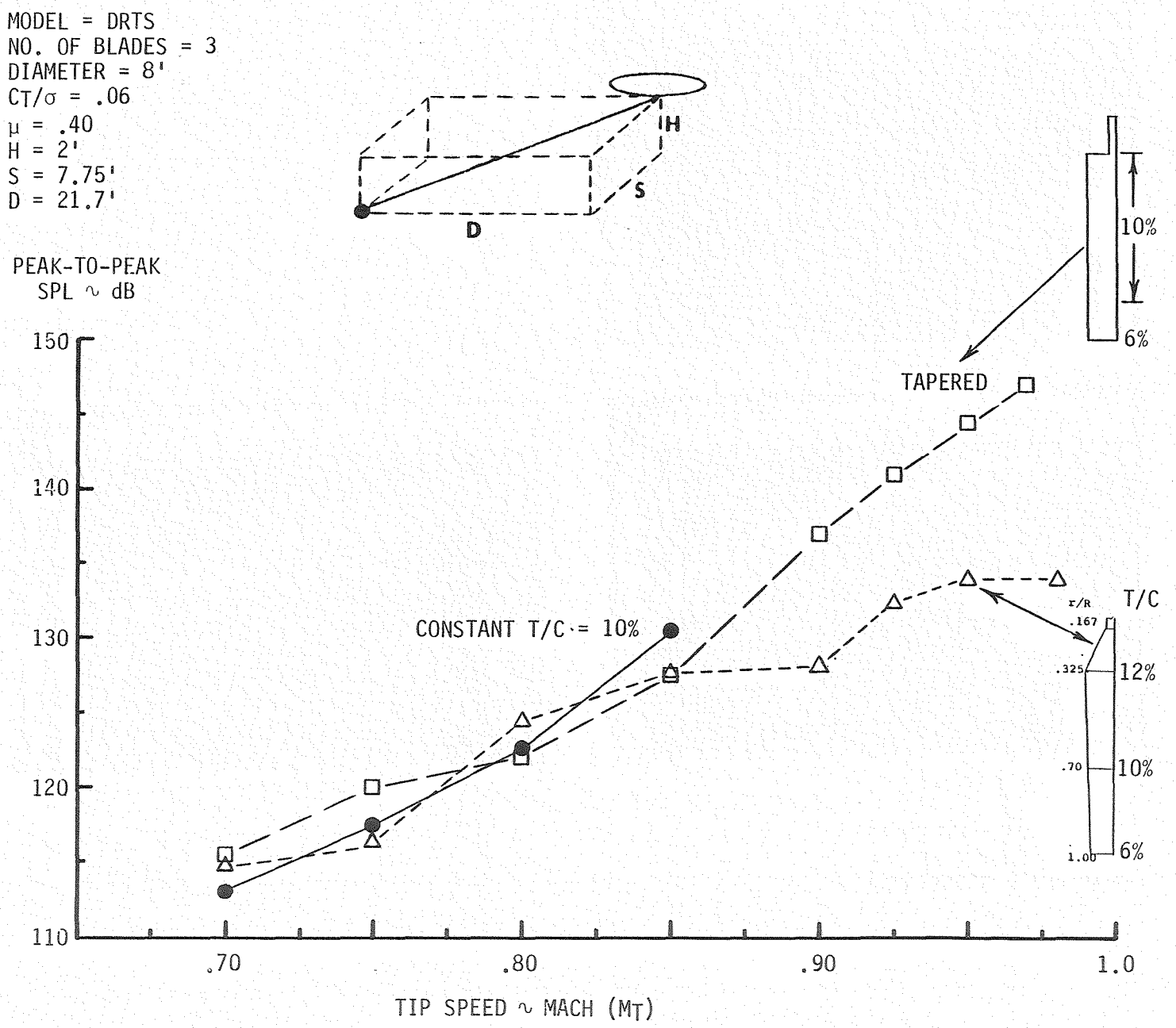

FIGURE 26. EFFECT OF ROTOR BLADE THICKNESS ON NOISE - MODEL DATA

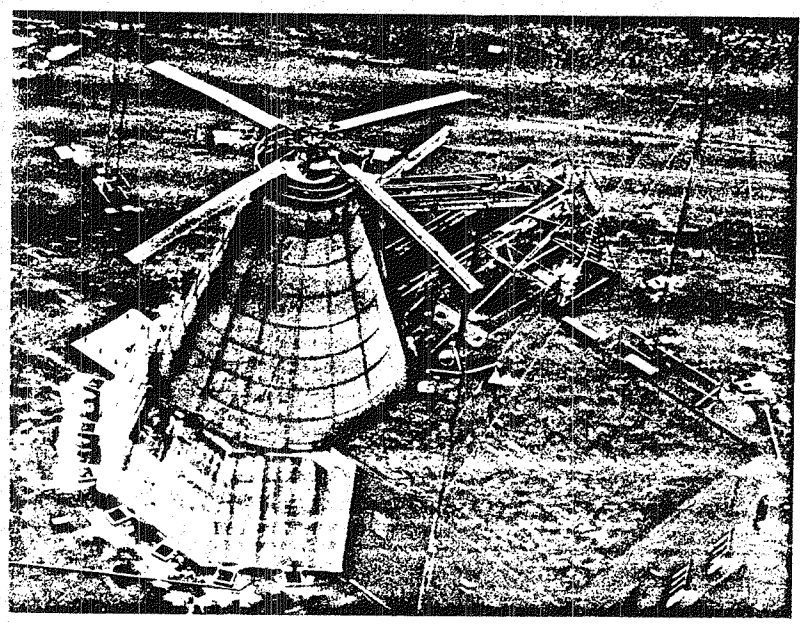

ROTOR TEST TOWER

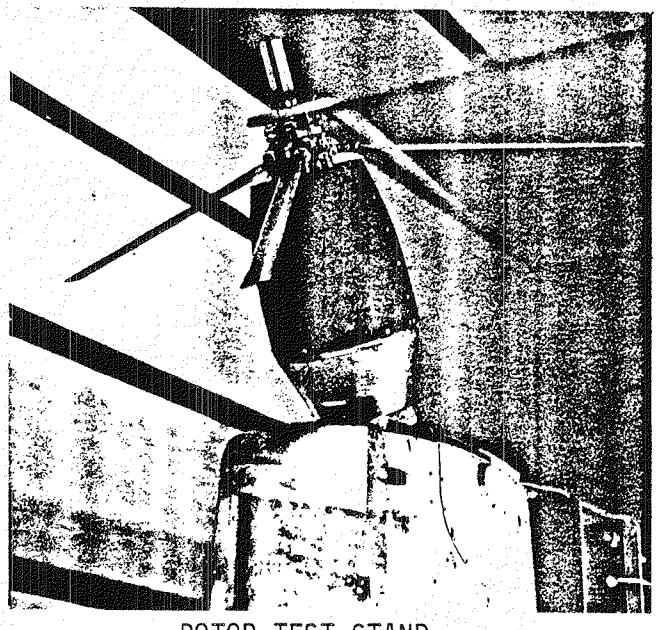

ROTOR TEST STAND

FIGURE 27. TEST ARTICLES - ISOLATED ROTOR EFFECTS

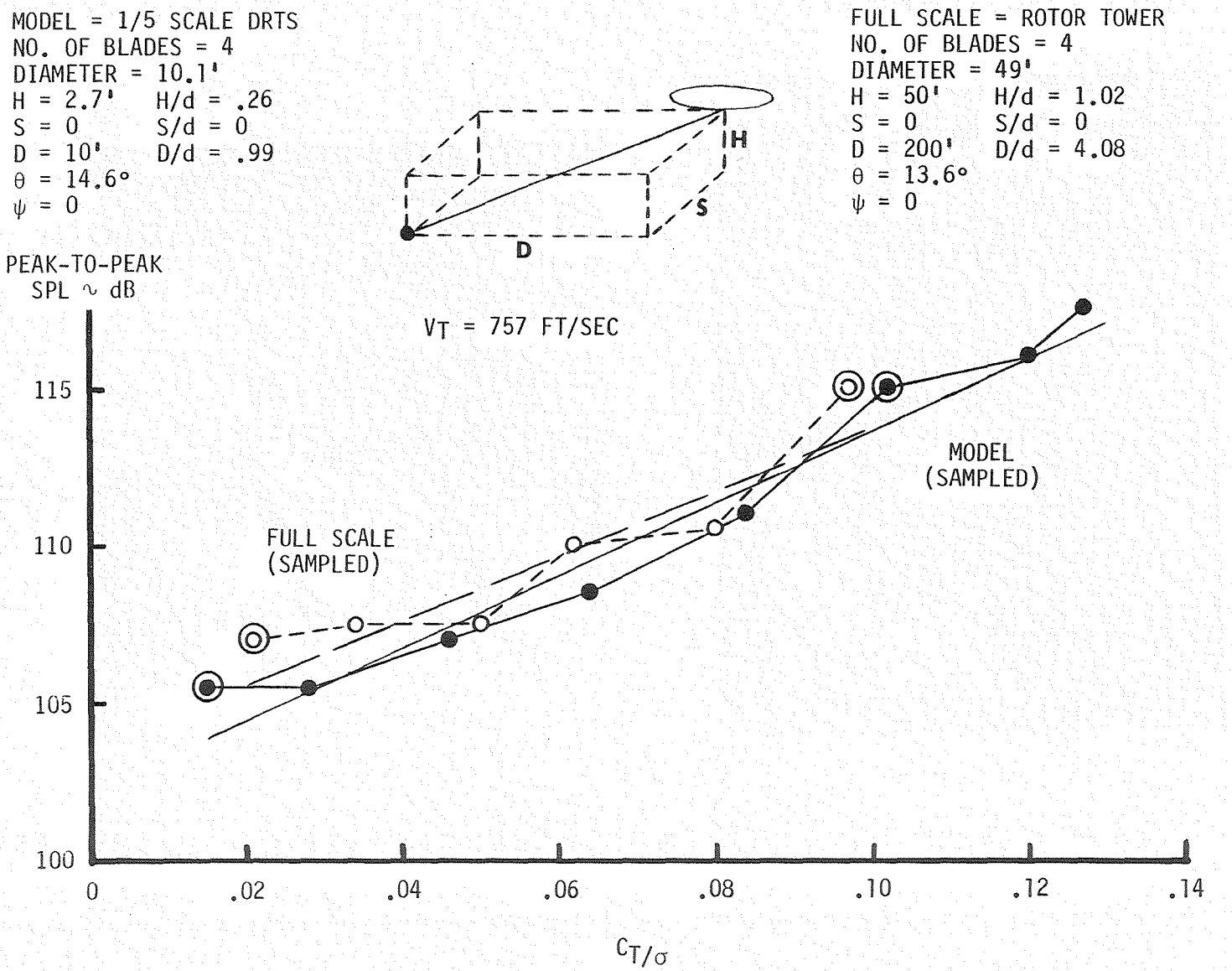

FIGURE 28A. COMPARISON OF MODEL AND FULL SCALE DATA IN HOVER - YUH-61A ROTOR - AMPLITUDE

FIGURE 28B. COMPARISON OF MODEL AND FULL SCALE DATA IN HOVER - YUH-61A ROTOR - WAVEFORMS

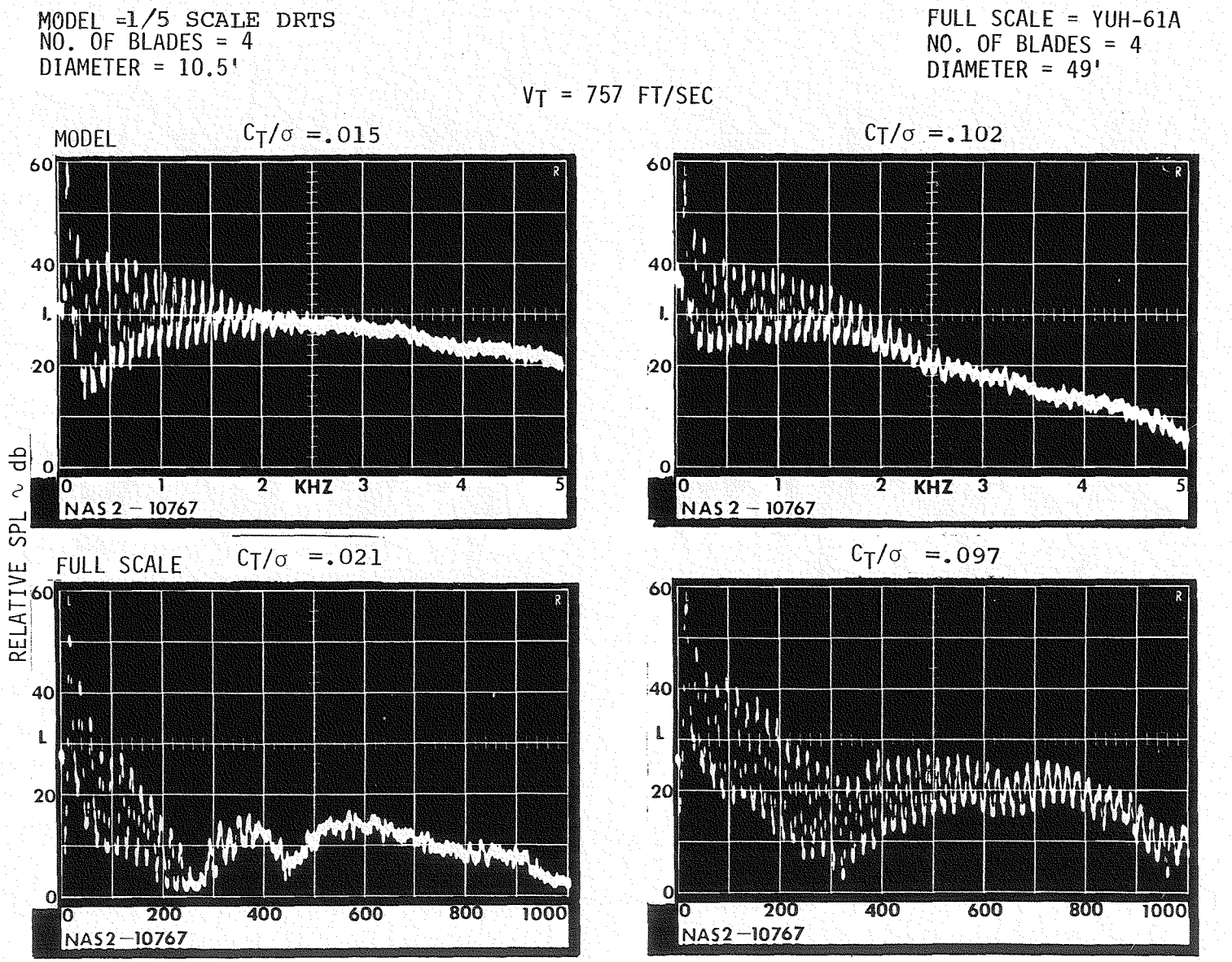

FIGURE 28C. COMPARISON OF MODEL AND FULL SCALE DATA IN HOVER - YUH-61A ROTOR - SPECTRA

FIGURE 29A. COMPARISON OF MODEL AND FULL SCALE DATA IN HOVER - MODEL 347 ROTOR - AMPLITUDE

FIGURE 29B. COMPARISON OF MODEL AND FULL SCALE DATA IN HOVER - MODEL 347 ROTOR - WAVEFORMS

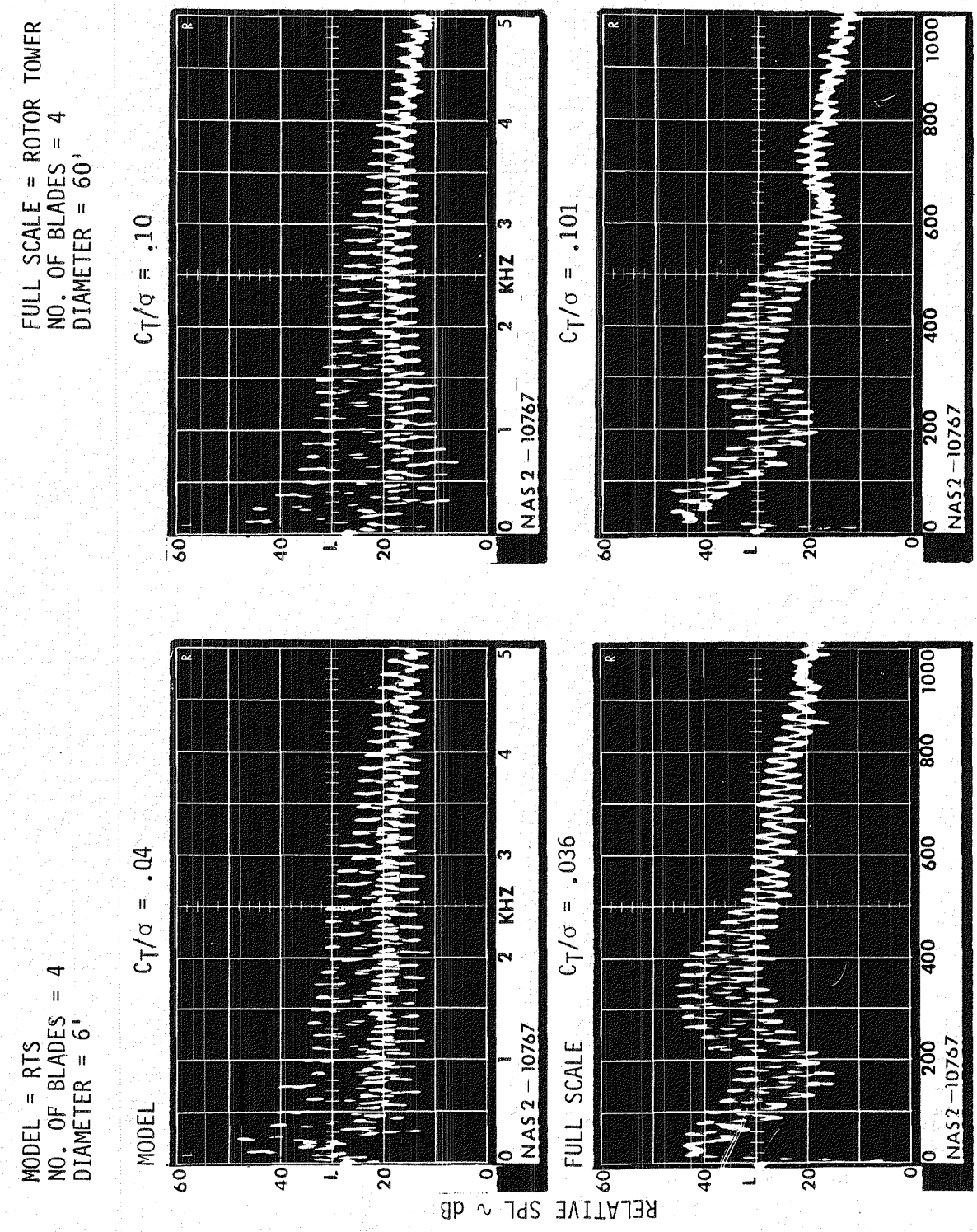

FIGURE 29C. COMPARISON OF MODEL AND FULL SCALE DATA IN HOVER - MODEL 347 ROTOR - SPECTRA

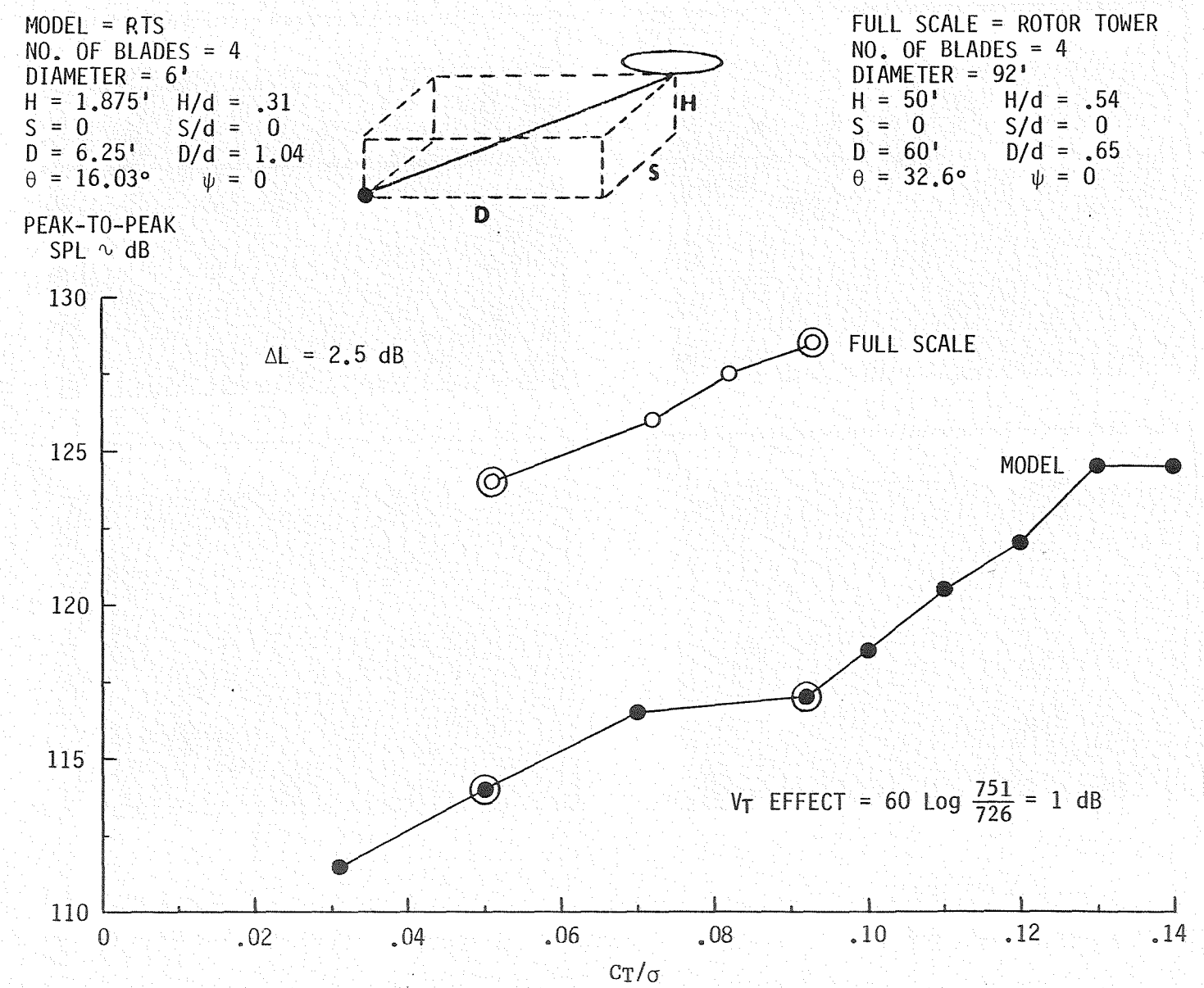

FIGURE 30A. COMPARISON OF MODEL AND FULL SCALE DATA IN HOVER - YUH-62 ROTOR - AMPLITUDE

FIGURE 30B. COMPARISON OF MODEL AND FULL SCALE DATA IN HOVER - YUH-62 ROTOR - WAVEFORMS

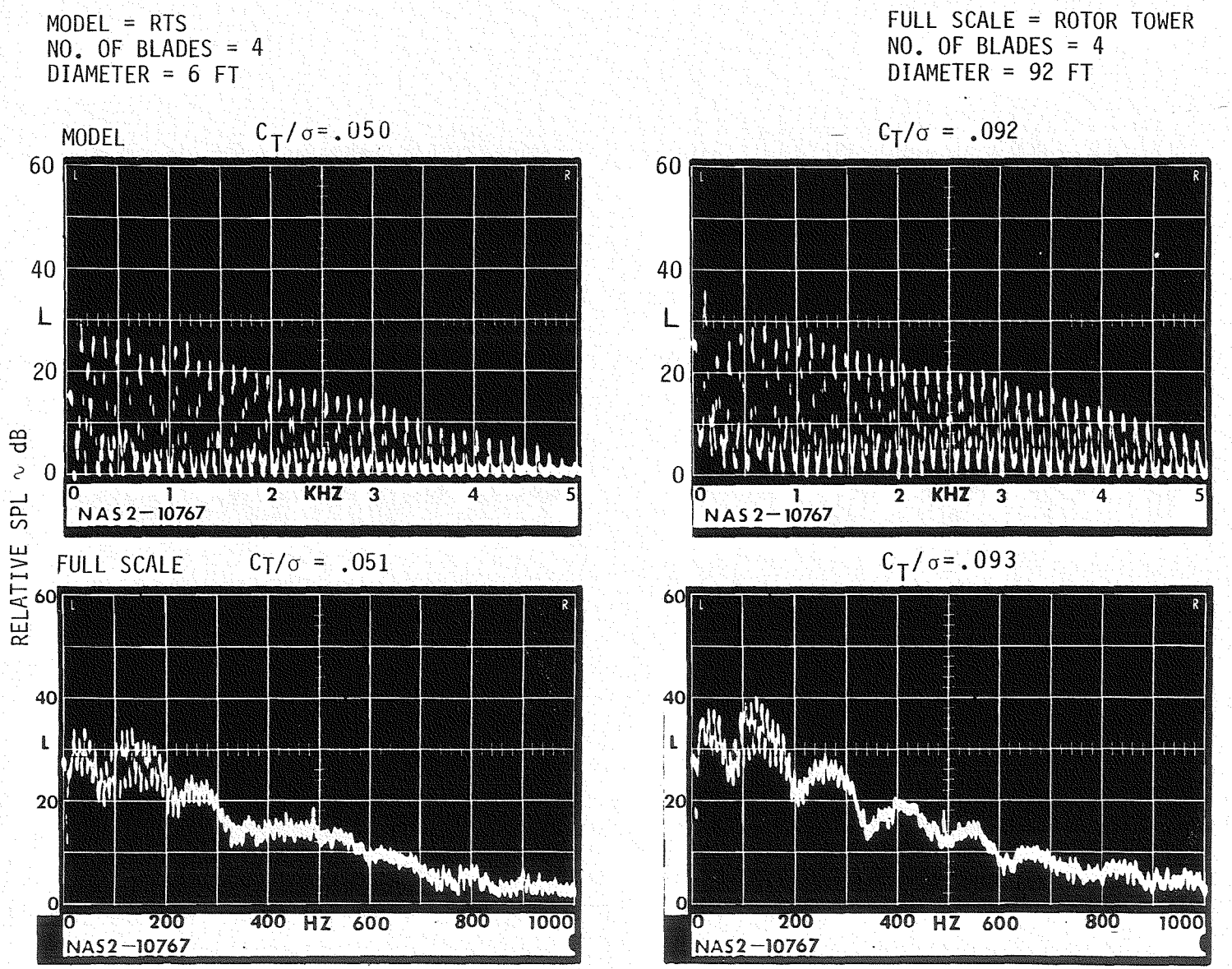

FIGURE 30C. COMPARISON OF MODEL AND FULL SCALE DATA IN HOVER - YUH-62 ROTOR - SPECTRA

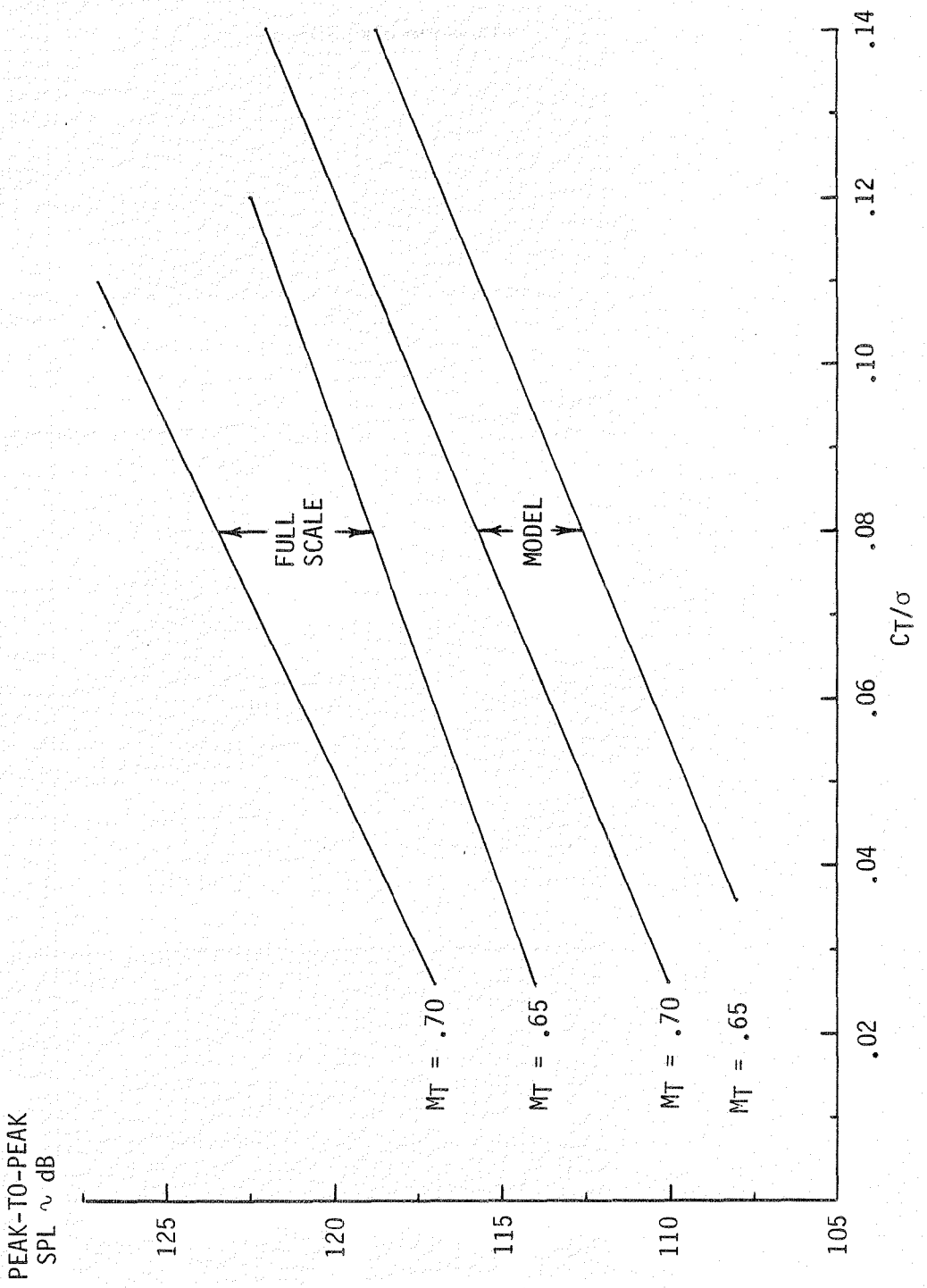

FIGURE 31. COMPARISON OF TIP SPEED EFFECTS IN HOVER - MODEL AND FULL SCALE DATA - ISOLATED ROTOR

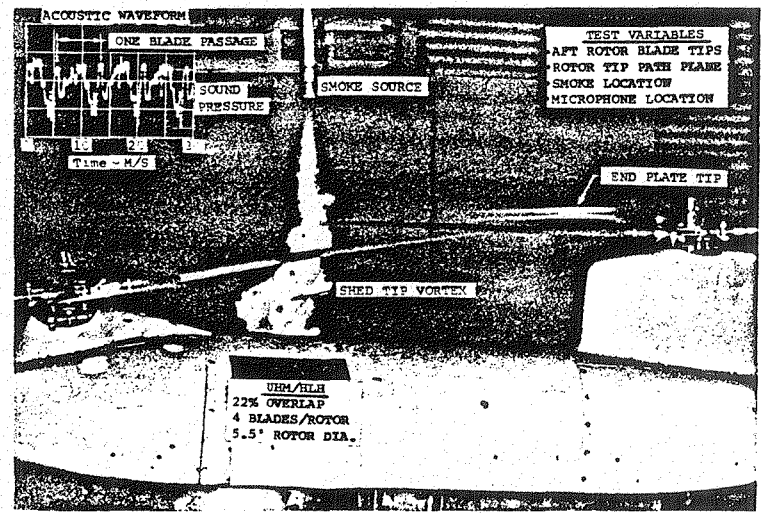

A

UNIVERSAL HELICOPTER MODEL

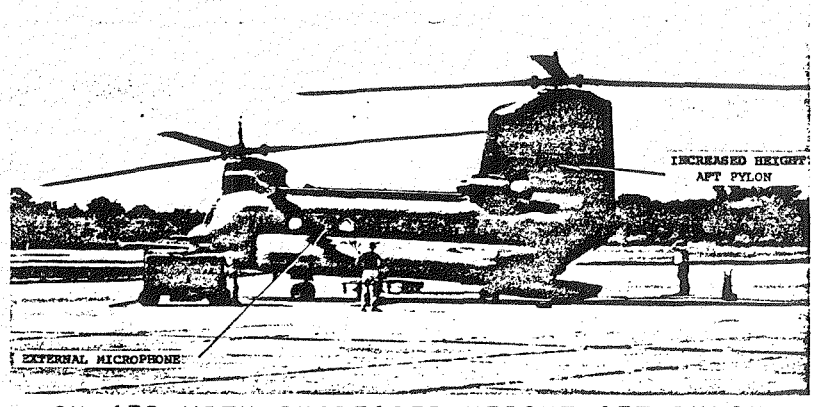

B

CH-47B WITH INCREASED HEIGHT AFT PYLON

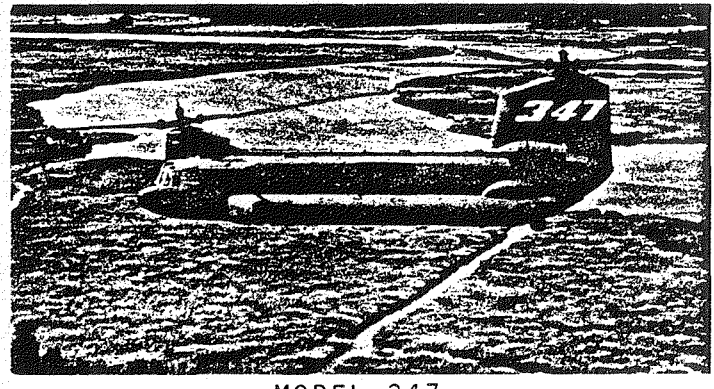

C

MODEL 347

FIGURE 32. TEST ARTICLES - TANDEM ROTOR EFFECTS

FIGURE 33A. COMPARISON OF MODEL AND FULL SCALE DATA - TANDEM ROTOR EFFECTS - 34% OVERLAP, 40 KTS - AMPLITUDE

FIGURE 33B. COMPARISON OF MODEL AND FULL SCALE DATA - TANDEM ROTOR EFFECTS - 34% OVERLAP, 40 KTS - WAVEFORMS

FIGURE 33C. COMPARISON OF MODEL AND FULL SCALE DATA - TANDEM ROTOR EFFECTS - 34% OVERLAP, 40 KTS - SPECTRA

FIGURE 34A. COMPARISON OF MODEL AND FULL SCALE DATA - TANDEM ROTOR EFFECTS - 34% OVERLAP, 80 KTS - AMPLITUDE

MODEL = UHM
NO. OF BLADES = 3
DIAMETER = 5.5'
V_T = 500 FT/SEC

FULL SCALE = CH-47B (HIGH PYLON)
NO. OF BLADES = 3
DIAMETER = 60'
V_T = 722 FT/SEC

TOTAL TRIM = 0°

TOTAL TRIM = 9°

TOTAL TRIM = 0°

TOTAL TRIM = 9°

FIGURE 34B. COMPARISON OF MODEL AND FULL SCALE DATA - TANDEM ROTOR EFFECTS - 34% OVERLAP, 80 KTS - WAVEFORMS

FIGURE 34C. COMPARISON OF MODEL AND FULL SCALE DATA - TANDEM ROTOR EFFECTS - 34% OVERLAP, 80 KTS - SPECTRA

FIGURE 35A. COMPARISON OF MODEL AND FULL SCALE DATA - TANDEM ROTOR EFFECTS - 34% OVERLAP, 120 KTS - AMPLITUDE

FIGURE 35B. COMPARISON OF MODEL AND FULL SCALE DATA - TANDEM ROTOR EFFECTS - 34% OVERLAP, 120 KTS - WAVEFORMS

FIGURE 35c. COMPARISON OF MODEL AND FULL SCALE DATA - TANDEM ROTOR EFFECTS - 34% OVERLAP, 120 KTS - SPECTRA

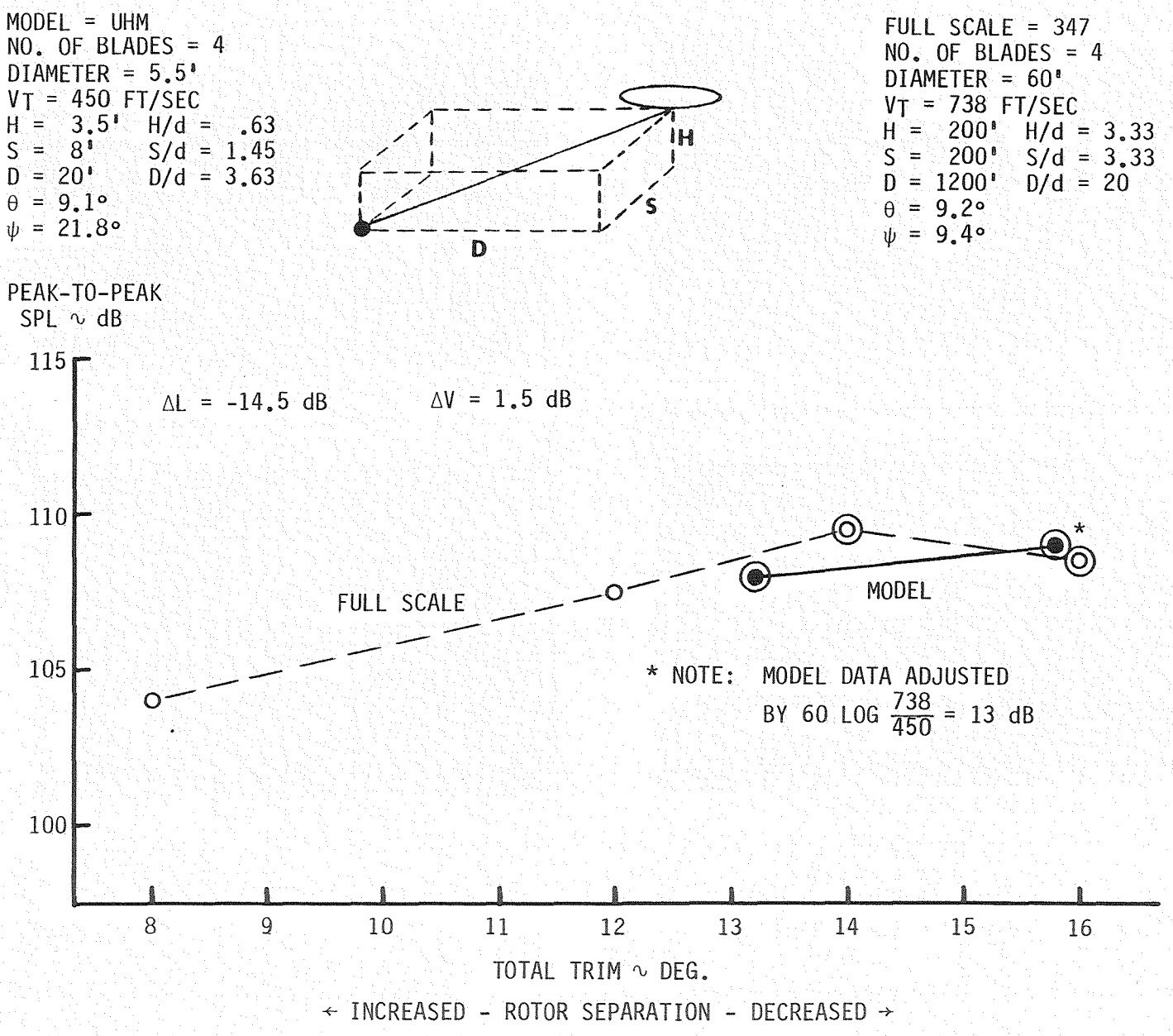

FIGURE 36A. COMPARISON OF MODEL AND FULL SCALE DATA - TANDEM ROTOR EFFECTS - 22% OVERLAP, 128 KTS - AMPLITUDE

FIGURE 36B. COMPARISON OF MODEL AND FULL SCALE DATA - TANDEM ROTOR EFFECTS - 22% OVERLAP, 128 KTS - WAVEFORMS

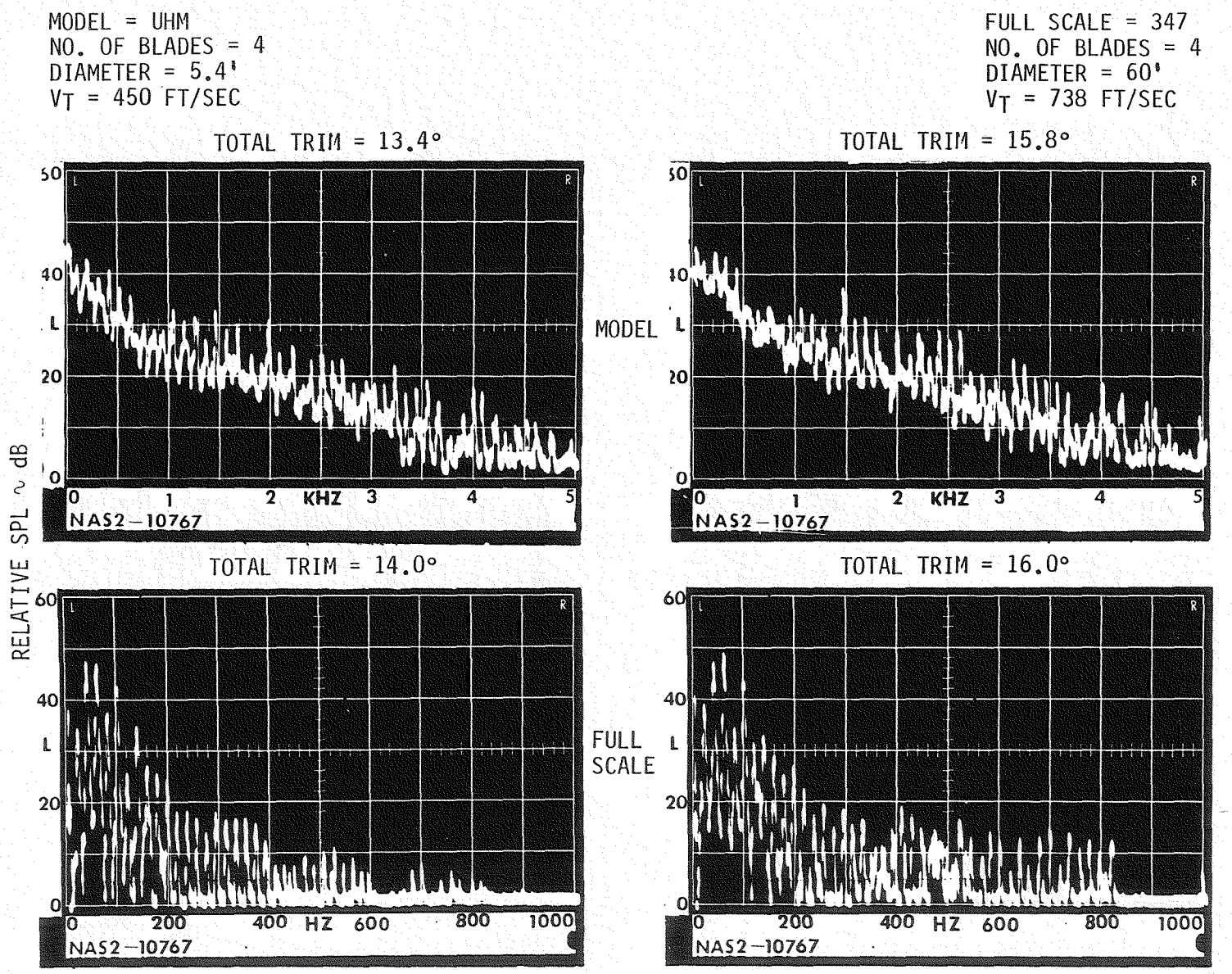

FIGURE 36C. COMPARISON OF MODEL AND FULL SCALE DATA - TANDEM ROTOR EFFECTS - 22% OVERLAP, 128 KTS - SPECTRA

FIGURE 37. EFFECT OF TANDEM OVERLAP - MODEL DATA

A

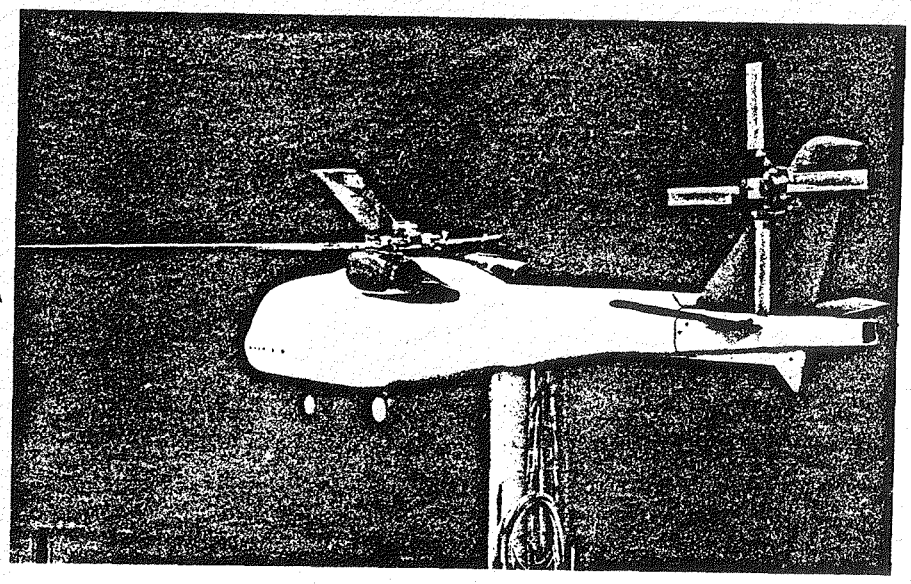

SINGLE ROTOR MODEL

B

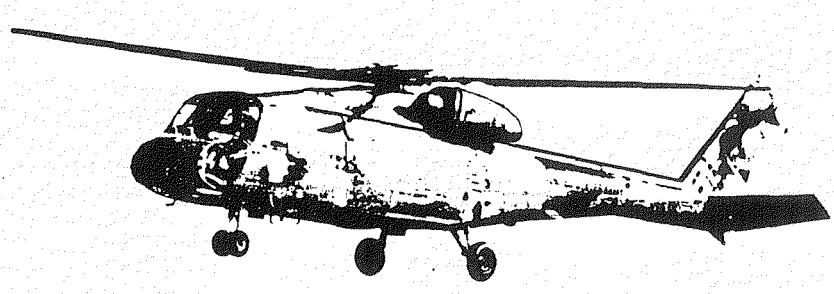

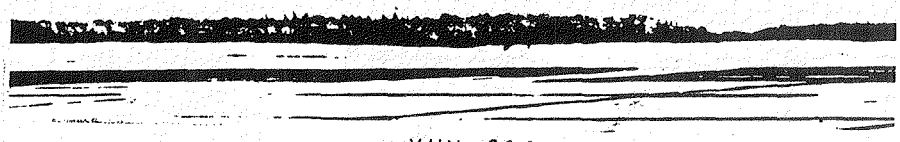

YUH-61A

FIGURE 38. TEST ARTICLES - MAIN/TAIL ROTOR INTERACTION

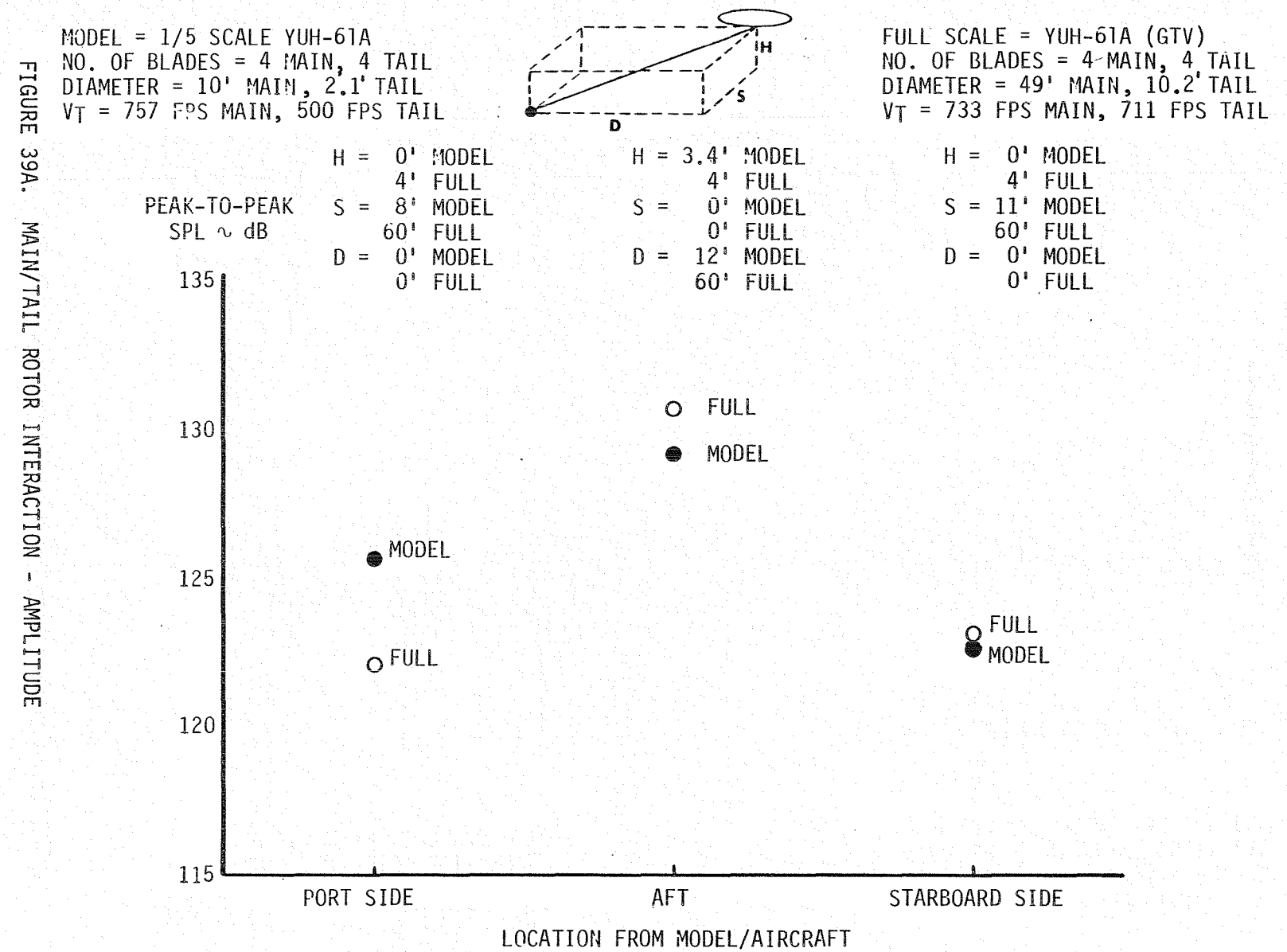

FIGURE 39A. MAIN/TAIL ROTOR INTERACTION - AMPLITUDE

MODEL = 1/5 SCALE YUH-61A
NO. OF BLADES = 4 MAIN, 4 TAIL
DIAMETER = 10' MAIN, 2.1' TAIL
V_T = 757 FPS MAIN, 500 FPS TAIL

FULL SCALE = YUH-62A (GTV)
NO. OF BLADES = 4 MAIN, 4 TAIL
DIAMETER = 49' MAIN, 10.2' TAIL
V_T = 733 FPS MAIN, 711 FPS TAIL

AFT

RIGHT SIDE

FIGURE 39B. MAIN/TAIL ROTOR INTERACTION - WAVEFORMS

MODEL = 1/5 SCALE YUH-61A
NO. OF BLADES = 4 MAIN, 4 TAIL
DIAMETER = 10' MAIN, 2.1' TAIL
V_T = 757 FPS MAIN, 500 FPS TAIL

FULL SCALE = YUH-62A (GTV)
NO. OF BLADES = 4 MAIN, 4 TAIL
DIAMETER = 49' MAIN, 10.2' TAIL
V_T = 733 FPS MAIN, 711 FPS TAIL

AFT

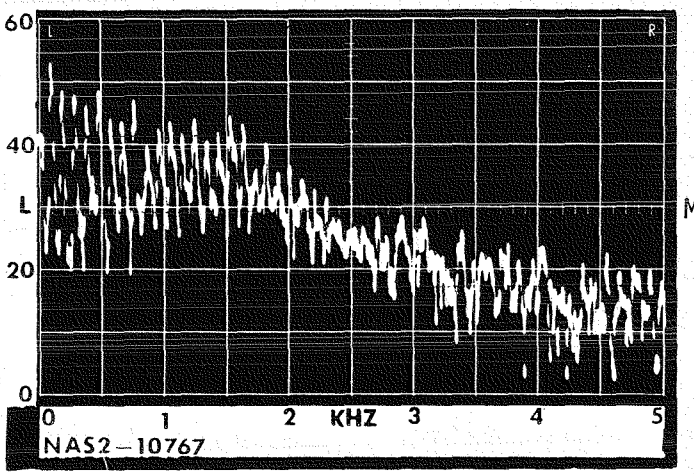

RIGHT SIDE

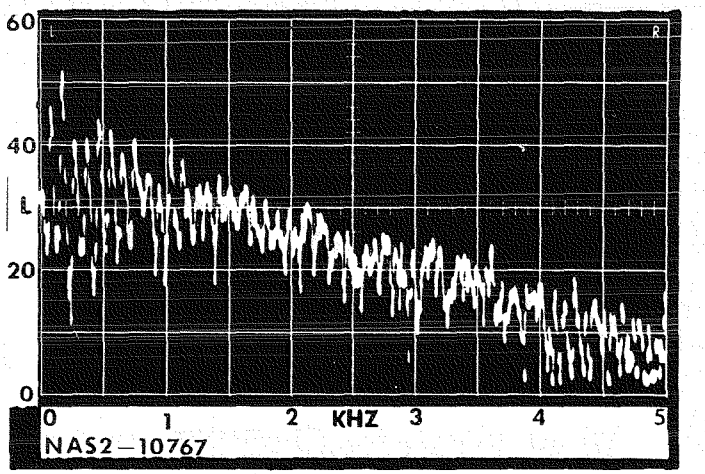

MODEL

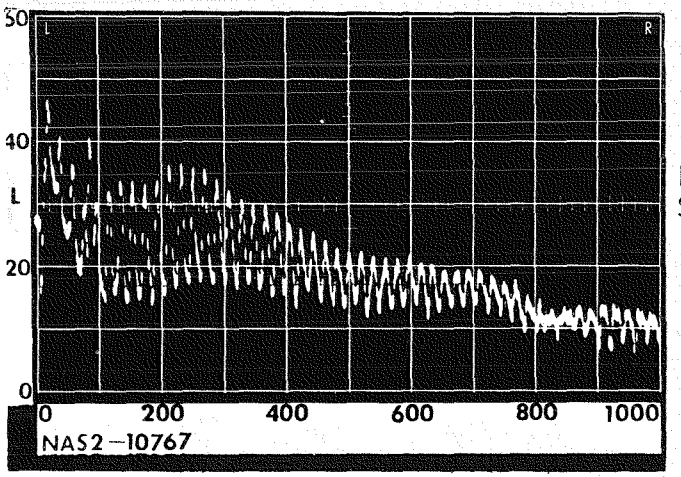

FULL SCALE

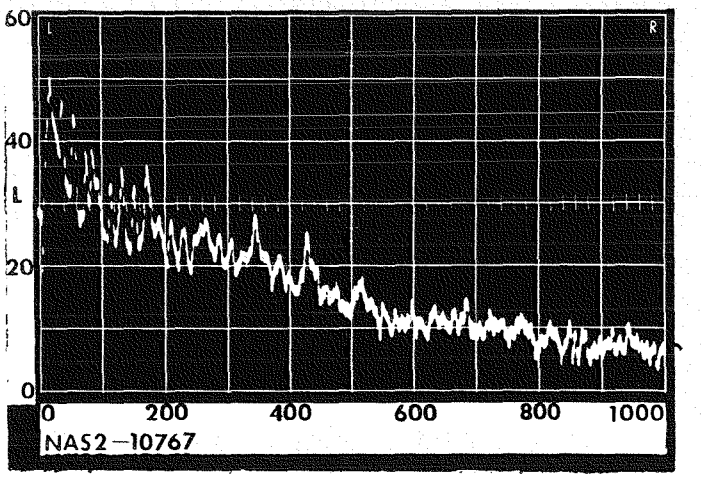

FIGURE 39C. MAIN/TAIL ROTOR INTERACTION - SPECTRA

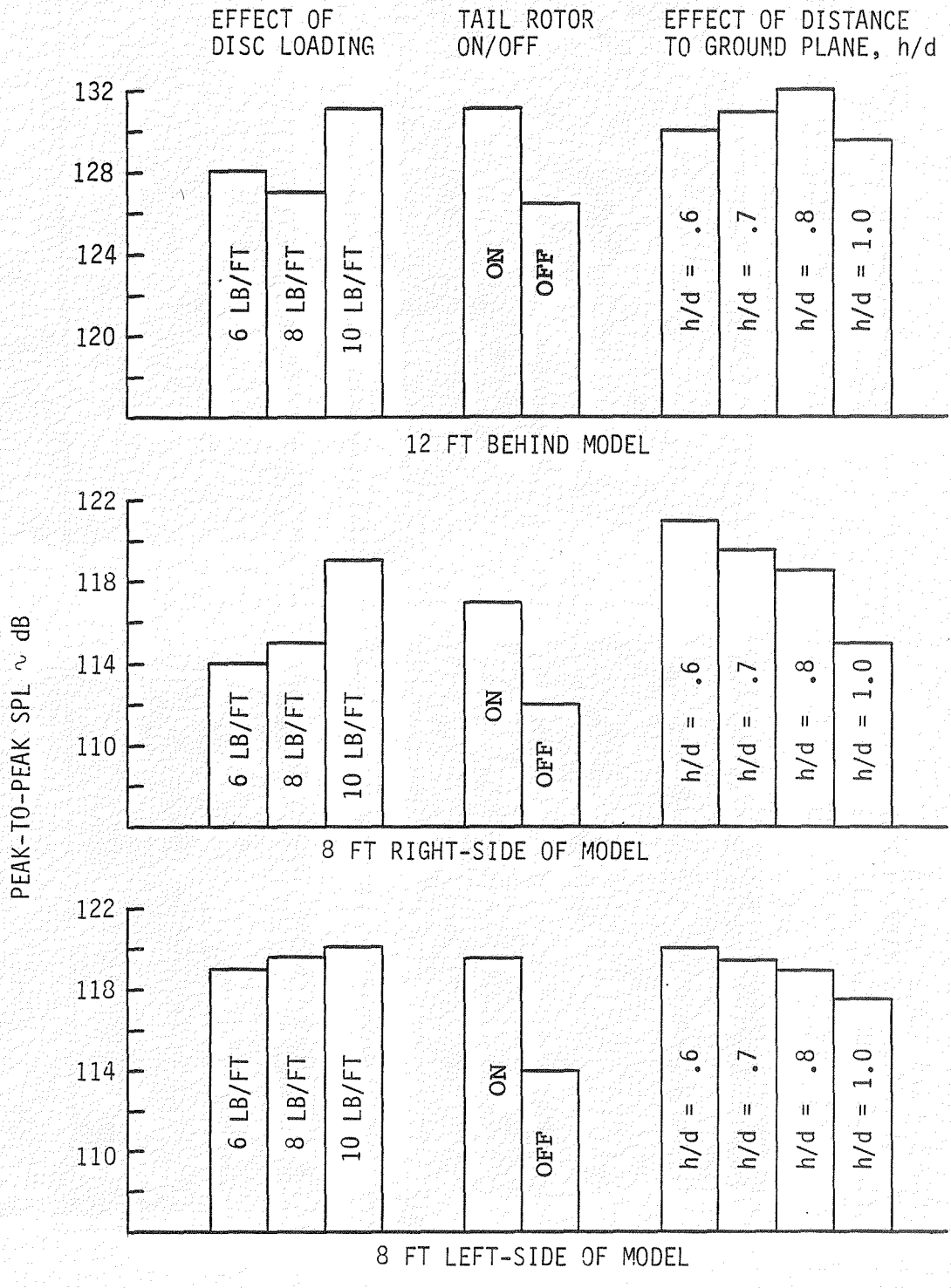

FIGURE 40. EFFECT OF OPERATING PARAMETERS ON MAIN ROTOR NOISE - MODEL DATA

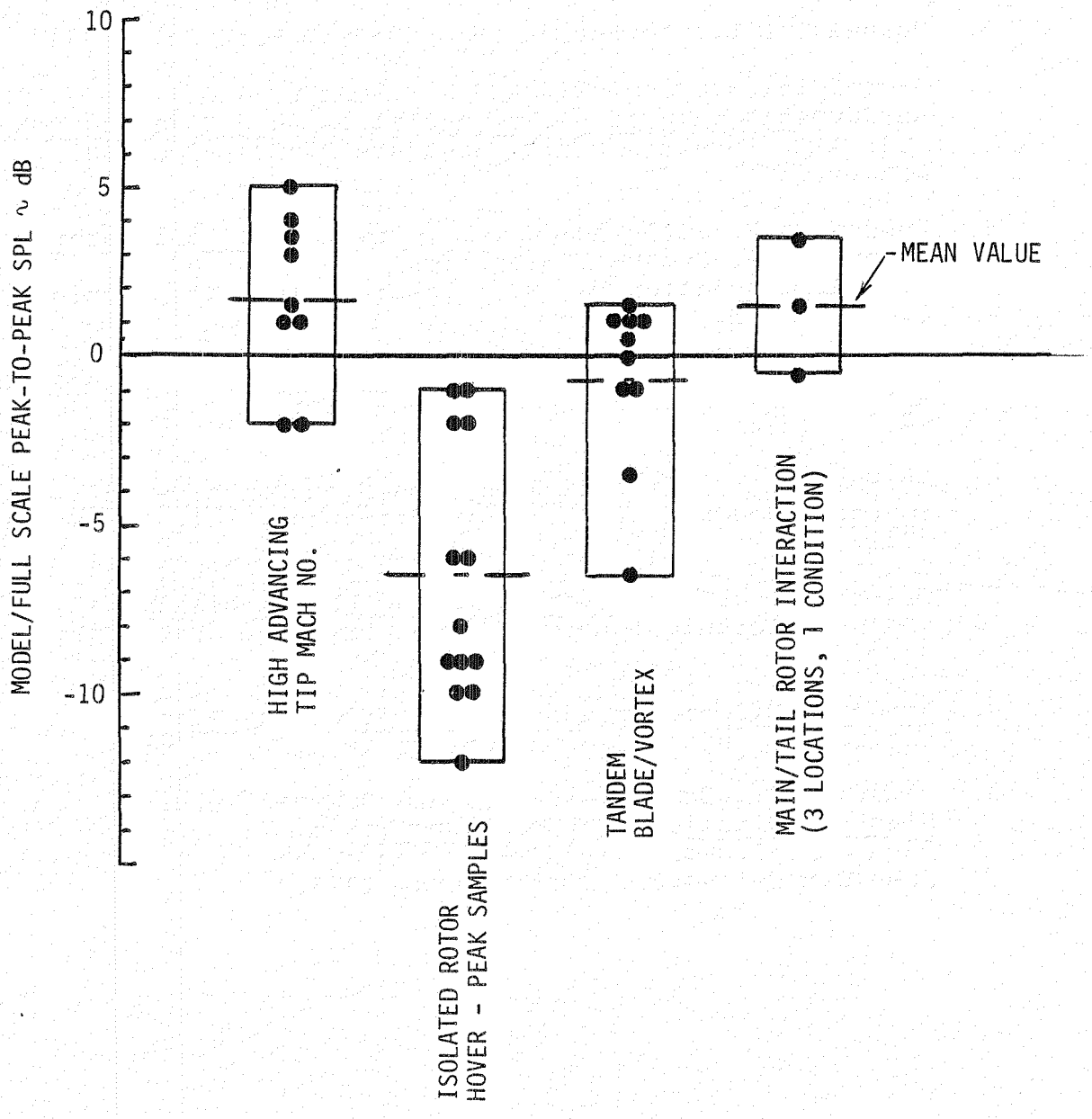

FIGURE 41. SUMMARY - COMPARISON OF MODEL AND FULL SCALE DATA

REFERENCES

1. Schmitz, F.H. and Boxwell, D.A., In-Flight Far-Field Measurements of Helicopter Noise, Journal of the American Helicopter Society, Volume 21, Number 4, October 1976.

2. Beranek, L.L., Acoustics, McGraw-Hill Book Co., 1954.

3. Sternfeld, H., Spencer, R.H., Schairer, J.O., An Investigation of Noise Generation on a Hovering Rotor, U.S. Army Research Office Contract DAHC04-69-C-0087, January 1971.

4. Lowson, M.V., Ollerhead, J.B., Studies of Helicopter Rotor Noise, USAAVLABS Technical Report 68-60, U.S. Army Aviation Material Laboratories, Ft. Eustis, Va. January 1969.

5. Hawkings, D.L., Lowson, M.V., Theory of Open Supersonic Rotor Noise, Journal of Sound and Vibration, Vol. 36, No. 1, 1974.

6. Wright, S.E., Discrete Radiation From Rotating Periodic Sources, Journal of Sound and Vibration, Vol. 17, No. 4, 1971.

7. Ollerhead, J.B., Helicopter Aural Detectability, USAAMRDL Technical Report 71-33, USAAMRDL, Ft. Eustis, Va. July 1971.

8. Acoustic Effects Produced by a Reflecting Plane, Society of Automotive Engineers AIR 1327, 1976.

9. Vause, C.R., Schmitz, F.H.,, and Boxwell, D.A.; High-Speed Helicopter Impulsive Noise, 32nd Annual National V/STOL Forum of the American Helicopter Society, May 1976.

1. Report No.	2. Government Accession No.	3. Recipient's Catalog No.
NASA CR-166337		

4. Title and Subtitle	5. Report Date
An Investigation of Rotor Harmonic Noise by the Use of Small Scale Wind Tunnel Models	6. Performing Organization Code April 1982
7. Author(s) Harry Sternfeld, Jr. Edward G. Schaffer	8. Performing Organization Report No.
	10. Work Unit No.
9. Performing Organization Name and Address Boeing Vertol Company P. O. Box 16858 Philadelphia, PA 19142	11. Contract or Grant No. NAS2-10767
	13. Type of Report and Period Covered Contractor Report Final Report
12. Sponsoring Agency Name and Address National Aeronautics and Space Administration Washington, D.C. 20546	14. Sponsoring Agency Code 505-42-21

15. Supplementary Notes
Technical Monitor: Marianne Mosher (415) 965-5044 or FTS 448-5044
M.S. 247-1
NASA Ames Research Center, Moffett Field, CA 94035

16. Abstract

Noise measurements of small scale helicopter rotor models were compared with noise measurements of full scale helicopters to determine what information about the full scale helicopters could be derived from noise measurements of small scale helicopter models. Comparisons were made of the discrete frequency (rotational) noise for 4 pairs of tests. Areas covered were tip speed effects, isolated rotor, tandem rotor, and main rotor/tail rotor interaction. Results show very good comparison of noise trends with configuration and test condition changes, and good comparison of absolute noise measurements with the corrections used except for the isolated rotor case. Noise measurements of the isolated rotor show a great deal of scatter reflecting the fact that the rotor in hover is basically unstable.

17. Key Words (Suggested by Author(s))	18. Distribution Statement
Helicopters, Rotors, Acoustics, Rotor Noise, Small Scale Tests, Wind Tunnel Tests, Noise	Unclassified - Unlimited

19. Security Classif. (of this report)	20. Security Classif. (of this page)	21. No. of Pages	22. Price*
Unclassified	Unclassified	100	

*For sale by the National Technical Information Service, Springfield, Virginia 22161

End of Document